NACA

RESEARCH MEMORANDUM

PRESSURE DROP IN COOLANT PASSAGES OF TWO AIR-COOLED TURBINE-BLADE CONFIGURATIONS

By W. Byron Brown and Henry O. Slone

Lewis Flight Propulsion Laboratory
Cleveland, Ohio

NATIONAL ADVISORY COMMITTEE
FOR AERONAUTICS

WASHINGTON
June 17, 1952

NACA RM E52D01

NATIONAL ADVISORY COMMITTEE FOR AERONAUTICS

RESEARCH MEMORANDUM

PRESSURE DROP IN COOLANT PASSAGES OF TWO AIR-COOLED TURBINE-BLADE CONFIGURATIONS

By W. Byron Brown and Henry O. Slone

SUMMARY

Pressure and temperature changes in the cooling air flowing through air-cooled gas-turbine blades have been measured experimentally in a static cascade on a 10-tube blade for both isothermal and nonisothermal flows, and on a 13-fin blade for isothermal flows. Values of pressure and temperature were obtained for a range of cooling-air flows corresponding to Reynolds numbers from 5,000 to 40,000; a Mach number range from 0.05 to 1.00; and for heat-transfer rates produced by ratios of hot-gas to blade-entrance cooling-air temperature from 3.08 to 0.57.

Friction coefficients were computed for all of the temperature ratios and the values were compared with values of friction coefficient calculated from von Kármán's equation for turbulent flow in smooth round pipes. When there was no heat transfer, the computed coefficients for the 10-tube blade agreed with those values calculated from the von Kármán equation. Friction coefficients obtained for the 13-fin blade were approximately 11 percent below the von Kármán values, but they were in agreement with friction coefficients obtained for small rectangular ducts of large aspect ratio. When heat transfer occurred, the friction coefficient decreased with increasing heat-transfer rates, in agreement with other NACA experiments. The friction coefficients were approximately 24 percent below the von Kármán values when the ratio of hot-gas to cooling-air temperature was 3.08.

In order to calculate an over-all pressure drop through an air-cooled blade and reduce the labor required in the numerical integration of the differential equation of momentum, simplified one-dimensional flow equations were developed for blades in static cascades and extended to blades in a rotating turbine. Over a range of blade spans from 2 to 6 inches, heat-transfer rates from 68 to 272 Btu per hour per square foot per $^{\circ}F$, and ratios of hot-gas to cooling-air temperature from 1.00 to 3.08, the errors in the computed blade-entrance pressures resulting from using these short-cut methods were within approximately 5 percent of the measured values. It was found that the value of friction coefficient that is required in the simplified and the exact flow equations may be determined from von Kármán's equation for isothermal flow in round pipes if

the error in the computed pressures may be as much as 6 percent. If greater accuracy is desired, von Kármán's value of friction coefficient may be corrected for the effect of heat transfer. A procedure for the calculation of an over-all pressure drop through an air-cooled blade is suggested, and a numerical example is presented wherein a blade-entrance static pressure is computed using the simplified flow equation for an air-cooled blade in a static cascade.

It was found that entrance losses to air-cooled turbine blades may be quite large, comparable with those inside the blade; they should be measured in any study of design performance.

INTRODUCTION

Air cooling of aircraft gas turbines is being investigated at the NACA Lewis laboratory to find low-alloy steels that may be substituted for the critically scarce high-temperature materials currently being used, and to find a means of increasing gas temperatures in order to provide substantial increases in specific power output. In many aircraft engine applications, the cooling air required for the engine would be bled from the engine compressor. In order to minimize the compressor work required for the cooling air and to keep the cooling-air temperature as low as possible, it is desirable to bleed the compressor at a point at which the pressure level is no higher than the required coolant-supply pressure. The factors which affect the required coolant-supply pressure and therefore the compressor bleed point are: (1) duct losses from the compressor to the turbine, (2) pressure ratio of the air as it passes through the turbine disk, (3) entrance losses at the entrance to the turbine blades, and (4) pressure losses through the turbine blades. The largest pressure losses are expected to occur through the blades and in the blade entrance sections; therefore, a knowledge of the methods for analytically evaluating these two losses would greatly reduce the experimentation required in determining blade losses and provide a design basis for cooling systems capable of efficient operation at the minimum coolant-supply pressure levels.

Some of the formulas required for calculating the pressure change between the root and the tip of air-cooled turbine blades as well as suggested experiments for securing the needed correlation data are given in reference 1. These formulas are based on the analyses of references 2 and 3, and the principal parameter involved in the formulas is the friction coefficient in the blade passage. Friction coefficients have not been previously measured in blade coolant passages or similar passage configurations. However, friction coefficients for isothermal fully developed turbulent flow in straight pipes have been studied extensively and are briefly summarized in reference 4. With the use of the equations for velocity distribution with fully developed turbulent flow, von Kármán (reference 5) predicts a relationship between friction coefficient and Reynolds number for smooth pipes which fits the experimental data.

Few data are available on friction coefficients for nonisothermal flow, although methods are suggested in references 4, 6, and 7, whereby the friction coefficient obtained for isothermal flow can be used for nonisothermal flow if the Reynolds number used in the correlation is based on special temperatures. Some data for rectangular air passages under nonisothermal conditions are presented in reference 8.

A pressure-drop investigation was undertaken on two air-cooled turbine-blade configurations in order to (1) determine experimental friction coefficients for both isothermal and nonisothermal flows and thus check the validity of using pipe friction coefficients in calculating air-cooled-blade pressure drops, (2) use the data to develop a simplified flow equation for calculating over-all pressure drops through air-cooled blades and thus eliminate the tedious step-by-step numerical integration of the flow equation reported in reference 3, (3) use the data to examine the magnitude of entrance losses which might be expected in the entrance sections of air-cooled blades, and (4) recommend a procedure that may be used for the calculation of air-cooled-blade pressure drops.

This investigation was conducted in a static cascade because a greater amount of instrumentation could be used. Pressure drops were measured experimentally for two air-cooled-blade configurations for isothermal and nonisothermal flows. A 10-tube blade was chosen for one of the blade configurations because such a blade appears to be promising and practical for air-cooled turbine rotors (references 9, 10, and 11). A 13-fin blade was chosen as the other blade configuration primarily because it has an internal cooling passage which is quite different from that of the 10-tube blade.

The results of this investigation are presented for a range of cooling-air flows giving Reynolds numbers from 5000 to 40,000; a Mach number range from 0.05 to 1.00; and for heat-transfer rates produced by ratios of hot gas to blade-entrance cooling-air temperature from 3.08 to 0.57 for the 10-tube blade; and for a ratio of hot gas to blade-entrance cooling-air temperature of 1.00 for the 13-fin blade.

ANALYSIS

General One-Dimensional Flow Equations

The general equations which give the pressure distribution in one-dimensional gas flow through a channel are stated and derived in reference 2. These general equations are adapted to the case of rotating blade coolant passages in reference 3, where the pressure distribution (in the notation of this report) is given by the equation

[redacted]

$$\frac{p}{p_{ex}} = \frac{A_{ex}}{A} \frac{M_{ex}}{M} \sqrt{\frac{T'}{T'_{ex}} \left(\frac{1 + \frac{\gamma-1}{2} M_{ex}^2}{1 + \frac{\gamma-1}{2} M^2} \right)} \tag{1}$$

(All symbols used in this report are defined in appendix A). Thus, the pressure at any point can be calculated from the values of blade flow area, Mach number, and total cooling-air temperature at that point.

The variation of Mach number of the air through the turbine blade coolant passage has been developed in reference 3. This variation, in the notation of the present report, is:

$$\frac{dM^2}{dy} = \frac{I_T}{T'} \frac{dT'}{dy} - I_f \left[\frac{4fb}{D_h} - \frac{I_R}{T'} \cdot \frac{2\omega^2 r_{in} b}{g^R} \left(1 + \frac{b}{r_{in}} - y \frac{b}{r_{in}} \right) \right] + \frac{I_A}{A} \frac{dA}{dy} \tag{2}$$

The terms I_T, I_f, I_R, and I_A are influence coefficients equal to

$$I_T = \frac{M^2(1 + \gamma M^2)(1 + \frac{\gamma-1}{2} M^2)}{1 - M^2} \tag{3}$$

$$I_f = \frac{\gamma M^4 (1 + \frac{\gamma-1}{2} M^2)}{1 - M^2} \tag{4}$$

$$I_R = \frac{1 + \frac{\gamma-1}{2} M^2}{\gamma M^2} \tag{5}$$

$$I_A = - \frac{2M^2 (1 + \frac{\gamma-1}{2} M^2)}{1 - M^2} \tag{6}$$

Because I_T, I_f, I_R, and I_A are functions of M only, the Mach number distribution can be found from equation (2) when the temperatures, friction coefficient, rotation, and blade geometry are known. Then, substitution of the Mach numbers in equation (1) will give the static-pressure distribution through the blade.

[redacted]

Determination of Experimental Blade-Passage Friction Coefficients

In order to check experimentally the validity of using pipe friction coefficients to compute pressure drops through air-cooled blades, the method discussed in reference 1 in conjunction with equation (2) can be used to determine a blade-passage friction coefficient. This operation consists of assuming a value of friction coefficient, solving equation (2) numerically for a blade entrance Mach number with an experimental value of blade exit Mach number, and then adjusting the value of the friction coefficient until the value obtained for the entrance Mach number agrees with the experimental value of entrance Mach number.

No heat transfer. - For the case of a stationary constant-coolant-passage-area blade with no heat transfer, the temperature, rotational, and area terms of equation (2) drop out and the resulting equation can be integrated directly to (see appendix B)

$$\frac{1}{M_{in}^2} = \frac{1}{M_{ex}^2} + 1.2 \ln \frac{M_{ex}^2}{M_{in}^2} \frac{1 + 0.2M_{in}^2}{1 + 0.2M_{ex}^2} + \frac{4fb\gamma}{D_h} \tag{7}$$

The value of γ is assumed to be 1.4 for the air passing through the blade. Thus, for the case of no heat transfer, a blade-passage friction coefficient can be determined from equation (7).

Heat transfer. - For the stationary constant-coolant-passage-area blade, with heat transfer, only the rotational and area terms of equation (2) drop out so that equation (2) may be written

$$\frac{dM^2}{dy} = \frac{I_T}{T'} \frac{dT'}{dy} - \frac{I_f 4fb}{D_h} \tag{8}$$

Even when reduced as in this case, equation (8) cannot be integrated in an exact closed form. It can, however, be integrated by the numerical methods reported in reference 3 and the blade-passage friction coefficient can be determined as explained in reference 1. For simplification, a linear variation of the total cooling-air temperature through the blade passage is assumed because it was shown in references 2 and 3 that the spanwise cooling-air temperature distribution curve is nearly linear.

Development of Simplified One-Dimensional Flow Equation for Calculation of Over-all Pressure Drop

The solution of equation (2) or (8), which is used in conjunction with equation (1) to obtain a pressure drop, involves a numerical integration which is quite tedious and time-consuming. Because in many cases only the over-all pressure change through the blade coolant passage is desired, a shorter method of obtaining the pressure change has been developed which dispenses with the step-by-step numerical integration of reference 3.

Simplified equation for static cascade. - When values of I_T and I_f are substituted in equation (8), an integration can be carried out (see appendix B for the derivation) resulting in

$$\frac{1}{M_{in}^2} = \frac{1}{M_{ex}^2} + 1.2 \ln \frac{M_{ex}^2}{M_{in}^2} \frac{1 + 0.2M_{in}^2}{1 + 0.2M_{ex}^2} + \frac{4fb\gamma}{D_h} + \gamma \ln \frac{T'_{ex}}{T'_{in}} + \frac{(T'_{ex} - T'_{in})}{\varphi} \left(\frac{1}{M^2T'}\right)_m \tag{9}$$

The parameter φ which is used to evaluate the integral $\int \frac{dT'}{M^2T'}$ between the blade entrance and the blade exit is a ratio of the arithmetic and true value of $\frac{1}{M^2T'}$ and is defined as (see appendix B)

$$\varphi = - \frac{\frac{1}{2}\left[\left(\frac{1}{M^2T'}\right)_{in} + \left(\frac{1}{M^2T'}\right)_{ex}\right]}{\frac{1}{T'_{ex} - T'_{in}} \int_{T'_{ex}}^{T'_{in}} \frac{dT'}{M^2T'}} \tag{10}$$

The distribution of M^2T', needed to evaluate the term under the integral sign, can be obtained from a numerical integration of equation (8). By this procedure, φ will be calculated for desirable ranges of M and T', and charts are presented in this report from which values of φ may be obtained for use in equation (9). These charts may be used for blade configurations and conditions similar to those of this investigation.

Simplified equation for rotating turbine. - For the case of a rotating turbine, wherein the blade flow area is assumed to be constant, the values of I_T, I_f, and I_R are substituted in equation (2) and an integration is carried out (see appendix B for the derivation) resulting in

[redacted]

$$\frac{1}{M^2_{in}} = \frac{1}{M^2_{ex}} + 1.2 \ln \frac{M^2_{ex}}{M^2_{in}} \frac{1 + 0.2M^2_{in}}{1 + 0.2M^2_{ex}} + \frac{4fb\gamma}{D_h} + \gamma \ln \frac{T'_{ex}}{T'_{in}} +$$

$$\frac{T'_{ex} - T'_{in}}{\varphi_\omega} \left(\frac{1}{M^2T'}\right)_m - \frac{2\omega^2 r_{in} b}{gR} \left(1 + \frac{\gamma-1}{2} M^2\right)_m \frac{1}{\varphi_\omega} \left(\frac{1}{M^2T'}\right)_m \left(1 + \frac{b}{r_{in}} \psi\right) \tag{11}$$

2512

The subscript ω indicates that φ is evaluated for a rotating turbine. It will be pointed out in a later section, however, that the effect of rotation on φ is negligible and that the charts of φ for static cascades can be used without introducing any appreciable error.

The parameter ψ is defined as (see appendix B)

$$\psi = \frac{\int_0^{1.0} \int_0^y \frac{dy}{M^2T'} dy}{\int_0^{1.0} \frac{dy}{M^2T'}} \tag{12}$$

This parameter is evaluated in a manner similar to φ and charts are presented in this report from which values of ψ may be obtained for use in equation (11). These charts may be used for blade configurations similar to those of this investigation.

Determination of Experimental Entrance Loss Coefficient

Aside from the pressure loss in the turbine blade, losses occur at other places in the air passage: at the entrance section to an air-cooled turbine blade; at contractions, enlargements, or obstructions; and at bends. The change in velocity or velocity distribution entails losses which in some cases comprise a relatively large part of the total loss and cause a considerable part of the resistance to flow. In this investigation, the entrance section to the air-cooled test blade is essentially a sudden contraction (see fig. 1). According to reference 4 (p. 122), the friction caused by a sudden contraction of the cross-sectional area of a pipe, or that at a sharp-edged entrance to a pipe, may be calculated from the formula

$$F = \frac{KV_{in}^2}{2g} \tag{13}$$

where F is the friction due to sudden contraction, foot-pound per pound of fluid; V_{in} is the average linear velocity downstream, feet per second; and K is the entrance loss coefficient which is a function of the ratio of the smaller cross-sectional area to the larger.

In order to calculate a value of K for the entrance section of the air-cooled test blades used in this investigation, equation (13) was rearranged as follows:

$$\Delta p' = \rho F = \frac{\rho K V_{in}^2}{2g} \tag{14}$$

where

$$V_{in} = \frac{w}{\rho A_B} \tag{15}$$

and

$$\rho = \frac{p_{in}}{RT_{in}} \tag{16}$$

When equations (15) and (16) are substituted in equation (14) (where $\Delta p' = p'_1 - p'_{in}$) and the result is divided by p_{in},

$$\frac{p'_1 - p'_{in}}{p_{in}} = K\left(\frac{w^2 T_{in}}{A_B^2 p_{in}^2}\right)\frac{R}{2g} \tag{17}$$

When equation (17) and experimental data are used, a curve can be plotted on logarithmic coordinates from which K can be determined.

APPARATUS AND INSTRUMENTATION

Equations (7), (8), and (17), presented in the ANALYSIS section, may be used to calculate the experimental blade-passage friction coefficients and an experimental entrance loss coefficient once the appropriate total and static pressures, the total cooling-air temperatures, the weight flow of the air passing through the blade, and the blade geometry are known. This investigation of friction coefficients and entrance losses for air-cooled blades was conducted in a static cascade wherein a greater amount of instrumentation could be installed than in an actual rotating turbine.

Test Facility

A sectional view of the blade test section used in this investigation is shown in figure 1. Combustion air passed successively through a flat-plate orifice, a combustor, a plenum chamber, the test section, and into the exhaust system. For the heat-transfer investigations, a gasoline combustor, which was capable of giving gas temperatures from 300° to 1000° F, was used. The inlet duct to the test section was equipped with a bellmouth to insure a uniform velocity profile at the entrance to the cascade. The setup was insulated against heat loss, from just downstream of the combustor to just downstream of the test section.

A cascade of seven blades was placed in the test section as shown in figure 2. The test blade, installed as the center blade, was the only blade through which air was passed. The other six blades had the same profile as the test blade. The air that was supplied to the test blade was obtained from the laboratory refrigerated air system; it could be heated by means of an electric heater in the supply line. The air passed successively through a plenum chamber, the entrance-blade extension, the test blade, the exit-blade extension, the plenum chamber, a flat-plate orifice, and then into the laboratory exhaust system (see fig. 1). Because it was impossible to connect the plenum chambers directly to the blade, entrance and exit blade extensions were used to conduct the air from the entrance plenum chamber to the test blade and from the test blade to the exit plenum chamber. The entrance-blade extension has a span of 6 inches and the exit-blade extension has a span of 3 inches. Both extensions have an internal free flow area of 0.043 square inch, a hydraulic diameter of 0.396 inch, and slots cut into their surfaces in order to reduce the amount of heat conducted from the hot test blade.

Blade Description

The air-cooled turbine blade configurations used in this investigation are a 10-tube blade and a 13-fin blade. Photographs showing the end views of the two blades are presented in figure 3. The geometric factors pertinent to the two blade configurations are given in the following table:

	10-tube blade	13-fin blade
Blade chord, in.	2.00	2.00
Outside perimeter, in.	4.35	4.53
Span, in.	3.92	3.50
Total free-flow area of internal cooling-air passage, sq in.	0.181	0.0962
Hydraulic diameter of internal cooling-air passage, in.	.103	.0670

[redacted]

10-tube blade. - The 10-tube blade used in this investigation was the same as the 10-tube blades used in the investigation reported in reference 9. The outside wall of the blade tapered linearly from the root to the tip for reduction of stresses during engine operation. The taper was not required for the cascade investigation, but it did not affect the results obtained. The nominal thickness of the wall at the tip was 0.040 inch and at the base, 0.070 inch. The blade shell was cast of high-temperature alloy X-40. The hollow blades were so cast that the core area was constant over the length of the blade. In order to increase the internal heat-transfer surface, 10 tubes were inserted in the hollow blade. They extended through the blade from tip to base. These tubes were brazed to each other and to the inside surface of the hollow blade by Nicrobraze. Of the ten tubes, four were 0.125-inch outside-diameter stainless steel with a wall thickness of 0.010 inch; and six were 0.156-inch outside-diameter low-carbon steel with a wall thickness of 0.0155 inch. The view of the blade tip (fig. 3) illustrates the tube arrangement. The blade span, 3.92 inches, was the same as that of the blades investigated in reference 9.

13-fin blade. - The 13-fin blade used in this investigation was originally designed for heat-transfer investigations in a static cascade. The blade was machined in two parts, and upon assembly the parts were welded together at the leading and trailing edges; therefore, the 13 cooling fins are not continuous (see fig. 3). The fins have an average thickness of 0.036 inch, and the average fin spacing is 0.046 inch. The blade was machined from high-temperature alloy S-816.

The 13-fin blade configuration had a span of 3.50 inches, which was shorter than the span of the 10-tube blade. The span was shorter because the blade was originally designed for a cascade of blades of this length. The difference in blade lengths does not affect the results of this investigation.

Instrumentation

In order to calculate friction coefficients for a blade coolant passage, it is necessary that the pressures and the temperatures of the air in the blade passage be known for a range of air flows. The instrumentation used in this investigation is shown in figure 1. Pressure taps and thermocouples were placed in the inlet and exit plenum chambers. Four static-pressure probes having an outside diameter of 0.030 inch were inserted into four representative passages of the test blade (see fig. 1). Two probes were used to measure the static pressure at the blade entrance, and two probes to measure the static pressure at the blade exit. The blade temperature distribution was measured by 11 thermocouples in the blade wall around the blade perimeter at the midspan.

In order to correct the cooling-air total temperatures measured in the plenum chambers for any heat picked up in the entrance- and exit-blade extensions so that the total cooling-air temperatures at the blade entrance and exit could be obtained, thermocouples were placed in the walls of the blade extensions. The entrance-blade extension had 12 spanwise thermocouples located at the midchord position and the exit-blade extension had 7 spanwise thermocouples also located at the midchord position. It was assumed that these thermocouples would give a representative integrated average of the wall temperatures of the two extensions.

The total temperature of the combustion gas was measured with three thermocouples located in the plenum chamber upstream of the test section. The air weight flow was measured by means of a flat-plate orifice downstream of the test section.

EXPERIMENTAL PROCEDURE

The operating conditions used in this investigation are listed in chronological order in table I. Note that no-heat-transfer investigations were conducted between heat-transfer investigations in order to provide a check on the experimental setup.

In order to calculate friction coefficients from equation (7) and (8), the cooling-air static pressures and total temperatures are required at the blade inlet and exit for a range of cooling-air weight flows. Pressure drops were obtained through the 10-tube and 13-fin blades for a range of air weight flows with no heat transfer, $T'_g/T'_{in} = 1.00$; and through the 10-tube blade with heat transfer, $T'_g/T'_{in} > 1.00$; and reverse heat transfer, $T'_g/T'_{in} < 1.00$. For the heat-transfer investigations, the gas-to-blade heat-transfer coefficient was held at approximately 136 Btu per hour per square foot per $^{\circ}F$ and the heat-transfer rate was varied by changing the temperature of the hot gas.

Static pressures were measured in the blades under investigation by inserting four static-pressure probes in four representative blade-coolant passages (fig. 1). In this way, two static-pressure readings, which were nearly identical, were obtained at the blade entrance and two readings at the blade exit. The two pressure readings at the blade entrance were averaged and the resulting value was assumed to be representative of the static pressure which would be obtained at the blade entrance if measurements were made in each blade coolant passage. This same procedure was applied at the blade exit.

Cooling-air total temperatures were measured in the entrance and exit plenum chambers. For the no-heat-transfer studies, these measured temperatures were assumed to be the same as those cooling-air temperatures which would exist at the blade entrance and exit. In the heat-transfer studies, however, the cooling air picked up heat as it passed through the entrance- and exit-blade extensions. Therefore, the temperatures that were measured in the plenum chambers were so adjusted that the resulting calculated temperatures were those occurring at the blade entrance and exit.

For the case of $T'_g/T'_{in} = 1.00$, the combustion-gas flow was supplied from the laboratory air system at approximately 100° F. The cooling air was heated so that the gas and cooling-air temperatures were approximately the same. A gasoline combustor was used when $T'_g/T'_{in} > 1.00$ so that the gas temperature could be varied from 300° to 1000° F. As before, cooling air was obtained from the refrigerated air system but in this case the cooling-air temperature was allowed to remain at the temperature at which it was supplied. After the cooling-air weight flow was set by adjustments in the blade pressure drop, frequent checks were made on the blade temperatures in order to ascertain when steady state conditions were reached. When the blade temperatures remained steady for approximately 15 minutes, the necessary readings were taken. For $T'_g/T'_{in} < 1.00$, the air passing through the coolant passage was heated to temperatures of 300° and 500° F and the combustion-gas flow remained at the temperature at which it was supplied, 100° F.

CALCULATION PROCEDURE

Once the blade entrance and exit Mach numbers and cooling-air total temperatures are determined from the data obtained in the static-cascade investigation, experimental friction coefficients may be determined. The calculation of friction coefficient requires that the distribution of M^2T' be determined for all of the conditions of the heat-transfer case. These distributions are also used to evaluate the parameters φ and ψ and the resulting values are used to construct the charts required for the solution of the simplified flow equations (9) and (11). In addition, the experimental data are used to determine an entrance loss coefficient for the air-cooled blades under investigation.

Method of Obtaining Experimental Blade-Passage Friction Coefficient

The experimental blade-passage friction coefficient is calculated by use of equations (7) and (8). In either equation, it is necessary to know the blade entrance and exit Mach numbers. These Mach numbers

are obtained from the following equation (reference 3)

$$I_c = \gamma M^2 \left(1 + \frac{\gamma-1}{2} M^2\right) = \frac{w^2 RT'}{A^2 g p^2} \tag{18}$$

The expression $\gamma M^2 \left(1 + \frac{\gamma-1}{2} M^2\right)$ is tabulated as the influence coefficient I_c in table I of reference 3; therefore, M can readily be determined from I_c once the right side of equation (18) is computed from experimental measurements.

No heat transfer. - Once values of the blade span, the hydraulic diameter, and the entrance and exit Mach numbers were known, experimental blade-passage friction coefficients for the no-heat-transfer studies were calculated from equation (7).

Heat transfer. - Friction coefficients were calculated from a numerical integration of equation (8) for the heat-transfer studies. Because of the effect of heat transfer, however, the cooling-air temperatures that were measured in the entrance and exit plenum chambers were not the values that would occur at the blade entrance and exit because the cooling air picks up heat as it passes through the entrance- and exit-blade extensions. Therefore, in order to calculate T'_{in} and T'_{ex} it is necessary to determine the amount of heat transferred from the walls of the entrance- and exit-blade extensions to the cooling air. In this way, the temperature rise of the cooling air $\Delta T'$ in the blade extensions can be computed. The following procedure is used to determine $\Delta T'$; for example, the heat transferred from the entrance-blade extension wall to the cooling air is given by:

$$q_3 = H_3 \, l_{i,3} \, b_3 (T_{w,3} - T'_{m,3}) \tag{19}$$

where $T_{w,3}$ is an integrated average wall temperature for the entrance-blade extension, $T'_{m,3}$ is the average cooling-air temperature in the entrance-blade extension, and the blade-to-coolant heat-transfer coefficient H_3 (in the notation of this report) is given by equation (4c) in reference 4 (p. 168) as

$$\frac{H_3 D_{h,3}}{k_3} = 0.023 \, Re_3^{0.8} \, Pr_3^{0.4} \tag{20}$$

[redacted]

where

$$Re_3 = \frac{wD_{h,3}}{A_3 \mu_3} \tag{21}$$

and

$$Pr_3 = \frac{c_{p,3}\mu_3}{k_3} \tag{22}$$

The gas properties are evaluated on the average cooling-air temperature in the blade extension.

Because

$$q_3 = wc_{p,3} \Delta T'_3 \tag{23}$$

equation (19) and (23) may be combined to give

$$\Delta T'_3 = \frac{H_3 l_{i,3} b_3 (T_{w,3} - T'_{m,3})}{wc_{p,3}} \tag{24}$$

The temperature rise of the cooling air in the entrance-blade extension is given by equation (24). In order to calculate $\Delta T'_3$, base the gas properties on T'_1 and then substitute the relationship $T'_{m,3} = \frac{1}{2} \Delta T'_3 + T'_1$ in equation (24). Once $\Delta T'_3$ is known, it can be added to T'_1 to obtain T'_{in}. This same procedure was applied to the exit-blade extension wherein $\Delta T'_4$ was subtracted from T'_2 to obtain T'_{ex}.

Once the static pressures and cooling-air total temperatures at the blade entrance and exit and the cooling-air weight flow through the blade are known, the Mach numbers at the blade entrance and exit may be determined as before from the relation given by equation (18). Then, the method discussed in reference 1 can be used to compute the friction coefficient f in equation (8). This method consists essentially in assuming a value of f, solving equation (8) numerically for M_{in} with a known starting value of M_{ex} and adjusting f until the value obtained for M_{in} agrees with the known observed value. The value of I_T and I_f are determined from table I of reference 3. A detailed method for solving equation (8) is presented in reference 3.

Method of Evaluating Parameters for Simplified Equations

The simplified one-dimensional flow equations (equations (9) and (11)) in conjunction with equation (1) may be used to calculate a blade-entrance static pressure once the exit Mach number, cooling-air temperature distribution, blade geometry, blade-passage friction coefficient, and equation parameters are known. The use of equations (9) and (11) for determining M^2_{in} involves some successive approximations because this unknown number occurs in the equation more than once, but it does not take long compared to the time required for the numerical integrations of equations (2) and (8). A sample calculation wherein equation (9) is used to compute a blade-entrance static pressure for a typical heat-transfer study is presented in appendix C. The use of equations (9) and (11) necessitates the evaluation of the parameters φ and ψ; the method of obtaining φ and ψ is therefore discussed in the following sections.

Evaluation of parameter φ for simplified equation. - The parameter φ may be determined from equation (10) once the distribution of M^2T' is known. Because this distribution may be obtained from a numerical solution of equation (8), and equation (8) was used to determine friction coefficients for the heat-transfer study, the parameter φ will be evaluated for the experimental data of this investigation.

When φ is calculated from equation (10), the integral $\int \frac{dT'}{M^2T'}$ may be written in the form $\frac{dT'}{dy}\int \frac{dy}{M^2T'}$ because dT'/dy is a constant value since the cooling-air temperature distribution curve was assumed to be linear in this investigation (y is a dimensionless number which is measured from the blade exit to the blade entrance). Therefore, when $\frac{dT'}{dy}\int \frac{dy}{M^2T'}$ is substituted in equation (10), the denominator of equation (10) becomes $\int_0^1 \frac{dy}{M^2T'}$ because $-dT'/dy = T'_{ex} - T'_{in}$. Thus, when the distribution of M^2 and T' is known for all of the heat-transfer studies, φ can be calculated from equation (10) for each of the points.

In order to determine the parameter φ in the case of no-heat-transfer studies, the integral $\int_0^1 \frac{dy}{M^2}$ which will appear in the denominator of equation (10) may be evaluated by the direct integration of equation (8).

Evaluation of parameter ψ for simplified equation. - The parameter ψ is determined from the experimental data of this investigation in the same manner that the parameter φ is determined. That is, a distribution of M is obtained from a numerical solution of equation (8) and the cooling-air temperature distribution is assumed to be linear. Then, ψ is evaluated from equation (12).

Method of Obtaining Experimental Entrance Loss Coefficient

An experimental entrance loss coefficient for the entrance section of the 10-tube blade is obtained by plotting equation (17) on logarithmic coordinates and determining K from the plot.

RESULTS AND DISCUSSION

The results of the experimental investigation of blade passage-friction coefficients for the two air-cooled blades are presented in figures 4, 5, and 6, and are discussed in the following sections of this report. Also, figures and discussions of the simplified flow equations and the effect of entrance losses are presented.

In presenting the results of this investigation, the parameter chosen to represent the heat-transfer effects is the ratio of the combustion-gas temperature to the blade entrance cooling-air temperature T'_g/T'_{in}. The parameter generally used in theoretical studies (see appendix D) is the ratio of the wall temperature to the temperature of the cooling air. In a practical design problem, the gas temperature is known and the cooling-air temperatures can be readily determined whereas the wall temperature is usually unknown and it is difficult to calculate. It will be shown later that a change of 100 percent in the test conditions of this investigation affects the computed blade entrance static pressure less than 5 percent. Therefore, the ratio T'_g/T'_{in}, although not an ideal parameter, can be used over an extensive practical range.

Experimental Blade-Passage Friction Coefficients

Friction coefficients were obtained for the no-heat-transfer studies so that the resulting values could be compared with values of the friction coefficient obtained for isothermal flow in round pipes. Reverse heat-transfer investigations were conducted in order to extend the data for determining the effect of heat transfer on friction coefficients.

No heat transfer. - The values of the friction coefficient f for the 10-tube and 13-fin blades, as determined from experimental data and equation (7), are plotted against Reynolds number in figure 4. The gas properties in the Reynolds number are evaluated by use of the average of the blade entrance and exit cooling-air temperatures; the characteristic dimension is the mean hydraulic diameter, that is, 4 times the total free-flow area divided by the total wetted perimeter.

Friction coefficients are compared with a curve computed from von Kármán's equation for turbulent flow in a smooth round pipe. This equation is (reference 5)

$$\frac{1}{\sqrt{f_{vK}}} = 4.0 \log \left(\mathrm{Re} \sqrt{f_{vK}} \right) - 0.40 \qquad (25)$$

Most of the values of f for the 10-tube blade are slightly above the von Kármán line, and a curve drawn through the points would lie 5 or 6 percent above the line. A table, based on the results of reference 12, is presented in reference 3 wherein the values of f obtained from von Kármán's equation may be corrected for entrance conditions when the length-to-diameter ratio is known. In the present case, the length-to-hydraulic-diameter ratio for the 10-tube blade is 38. The table in reference 3 gives a ratio of $f/f_{vK} = 1.05$ for a length-to-diameter ratio of 40. Therefore, if the values of f which were obtained for the 10-tube blade had the entrance effects eliminated according to reference 3, they would be reduced approximately 5 percent and the agreement between the 10-tube blade values of f and von Kármán's line would be improved.

All of the values of f for the 13-fin blade fall below the von Kármán line, about 10 percent on the average. The length-to-diameter ratio is 52 for this blade; therefore, the ratio of f/f_{vK} is about 1.01 by extrapolation from reference 3. Consequently, the values of f for the 13-fin blade would lie approximately 11 percent below the von Kármán line when entrance effects are considered. This behavior of f has been observed in reference 8 wherein friction coefficients were determined for three different rectangular ducts having gaps between the side walls of 9/16, 1/4, and 1/8 inch. In turbulent flow, at a given Reynolds number, it was observed that f decreased as the gap between the walls decreased. For the 1/8-inch-gap duct, which has a large aspect ratio, the experimental values of f were approximately 12 percent below the line for turbulent flow in smooth round pipes as shown in figure 4. These results were attributed to the narrowness of the rectangular ducts. That is, in turbulent flow, a large part of the pressure drop is caused by eddy formations, and anything which tends to reduce these formations should also act to reduce friction loss. The results of this investigation show the same trend as the results reported in reference 8.

Heat transfer. - The values of f for the 10-tube blade with heat transfer are plotted against Reynolds number in figure 5. Each part of figure 5 represents a different temperature ratio and therefore a different rate of heat transfer. (The temperature ratio T'_g/T'_{in} is used only to signify a rate of heat transfer.) All of the values of f for heat transfer are compared with von Kármán's line. Comparison of parts (a) to (e) of figure 5 shows that when the temperature ratio is 0.57, most of the values of f are above the von Kármán line. As the temperature ratio increases gradually to 3.08, the values of f move downward until at a ratio of 3.08, most of them are approximately 24 percent below the von Kármán line. Therefore, as the temperature ratio and thus the heat-transfer increases, the air-cooled-blade coolant passage friction coefficient shows a distinct downward trend from the friction coefficients obtained for the case of no heat transfer.

In order to separate the temperature trend from the Reynolds number effect, advantage is taken of the fact that over a limited range of Reynolds numbers, 5000 to 200,000 (reference 4), f varies inversely as $Re^{0.2}$. Thus, over the range of this investigation, the product $fRe^{0.2}$ should be constant when there is no heat transfer, and any changes in this product will be due to the effect of heat transfer. In figure 6, $fRe^{0.2}$ is plotted against temperature ratio and all of the points at a single temperature ratio are averaged. The result is the line shown in figure 6, the equation for which is

$$fRe^{0.2} = 0.0483 \left(T'_g/T'_{in}\right)^{-0.189} \tag{26}$$

When deviations from the line of the individual observed points are used to calculate the probable error of a single observation, and when this probable error is plotted above and below this line, the two dashed lines shown in figure 6 are determined. Thus, if all of the 94 data points used determine the line were plotted, half of them would be inside the dotted lines and half would be outside.

This same trend, a decrease of friction coefficient with an increase of the rate of heat transfer to the air stream for turbulent flow, is reported in an investigation on a single round tube (reference 13). Boundary-layer theory, as is shown in appendix D, confirms this behavior. That is, according to the table in appendix D, the friction coefficient should decrease as the rate of heat transfer to the cooling air increases for turbulent flow. Therefore, when the wall is hotter than the cooling air, the value of f calculated from von Kármán's equation (equation (25)) should be corrected by a temperature factor which in the present case is $\left(T'_g/T'_{in}\right)^{-0.189}$.

Accuracy of Calculated Blade-Entrance Static Pressures When Friction Coefficients Used are Other Than Exact Values

In the calculation of air-cooled-blade pressure drops, it is important to know whether or not ordinary pipe correlations can be used in determining a friction coefficient. Also, it is desirable to know how sensitive the calculated pressure is to errors in the value of f used in the flow equations.

Effect of von Kármán friction coefficients on computed pressures. - The effect on computed pressures of using the von Kármán friction coefficients was checked by calculating blade-entrance static pressures for all of the data points obtained for the 10-tube blade at a temperature ratio of 3.08. Equations (9) and (1) were used to compute pressures; the friction coefficient was determined with (a) a value of f calculated from von Kármán's equation (equation (25)) and (b) a value of f corrected to account for the heat-transfer effect, that is, $f = f_{vK}/(T'_g/T'_{in})^{-0.189}$. The results of these calculations are presented in figure 7 where the ordinate is the percentage error between calculated and measured pressures, and the abscissa is the measured static pressure at the blade entrance. For the first case wherein f_{vK} is used in equation (9) (fig. 7(a)), the largest errors that occurred are about 6 percent; most of them are much less. For the second case wherein a corrected value of f is used in equation (9) (see fig. 7(b)), the largest deviations are about 3 percent. In both cases, some of the error obtained may be attributed to errors in the experimental measurements of the static pressures. Thus, for cases where a maximum error of about 6 percent is tolerable for the calculated pressure at the blade entrance, the ordinary von Kármán value of f can be used in equation (9). If more precision is desired, f_{vK} should be corrected by a temperature-correction factor.

Effect of error in friction coefficient on computed pressures. - As a further step, the effect of error in the friction coefficient on the computed pressures was investigated. Calculations of blade-entrance static pressures were made with values of f in equation (9) which differ from the exact data point value of f by ±20 percent. The exact value of f was obtained from experimental measurements and equation (8); consequently, calculations showing the effect of variations in f are not affected by experimental errors. These calcalations, in which f was changed by 20 percent, were made for high exit Mach numbers where the effect of friction coefficient is the greatest. With the largest heat-transfer rate ($T'_g/T'_{in} = 3.08$), the resultant change in pressure was approximately 3 percent. In the case of no heat transfer, the presure change was approximately 5 percent. Thus, moderate errors in f would not be serious in many applications when blade-entrance static pressures are calculated.

Evaluation of Parameters for Simplified Equations

In practice, equations (9) and (11) can be used for calculating the blade-entrance Mach number M_{in} when the blade-exit Mach number M_{ex}, the friction coefficient f, the blade span, the hydraulic diameter, the entrance and the exit cooling-air temperatures T'_{in} and T'_{ex}, the angular velocity, and the distance from the turbine center line to the blade entrance are known. Once M_{in} is computed, the blade-entrance static pressure can be calculated from equation (1). Because the use of equations (9) and (11) requires a knowledge of the parameters φ and ψ, these parameters must be evaluated.

Experimental evaluation of φ for simplified equation. - For the range of variables covered in this investigation, values of φ were calculated for all of the heat-transfer and no-heat-transfer data points by use of equation (10). The values of φ, which varied from about 0.89 to 1.14, were plotted against M_{ex} in figure 8(a). Each temperature ratio or heat-transfer rate produced a separate curve. The curves in figure 8(a) are too far apart for interpolating conveniently; therefore, a cross plot was made in figure 8(b) where φ was plotted against temperature ratio for a series of constant values of M_{ex}. The experimental data used in evaluating φ were obtained in the 10-tube blade. Therefore, figures 8(a) and (b) can be applied to a blade having a span approximately the same as that of the 10-tube blade (3.92 in.) and having the same heat input. For a blade having an external configuration similar to the 10-tube blade, the outside heat-transfer coefficient would be approximately 136 Btu per hour per square foot per $^{\circ}F$. The effect of changes in blade span and heat-transfer rate on φ will be discussed in a subsequent section.

Experimental evaluation of ψ for simplified equation. - For the range of variables covered in this investigation, values of ψ were calculated for all of the heat-transfer and no-heat-transfer data points by use of equation (12). Values of ψ, which varied from about 0.36 to 0.50, were plotted against M_{ex} in figure 9(a) for four temperature ratios. For convenience, a cross plot of figure 9(a) is presented in figure 9(b) where ψ is plotted against T'_g/T'_{in} for constant blade-exit Mach numbers. The data used in evaluating ψ were obtained only on the 10-tube blade.

Influence of blade span and outside heat-transfer coefficient on φ. - The parameter φ, which must be used in the simplified one-dimensional flow equations, was obtained from experimental results for the 10-tube blade. It is interesting to know, however, how φ varies with blade span and heat-transfer rate. Therefore, φ was evaluated

analytically for blades having spans shorter and longer than that of the 10-tube blade, and for blades having an outside heat-transfer coefficient half as large and twice as large as that obtained for the 10-tube-blade heat-transfer investigations.

The blade span of the 10-tube blade was 3.92 inches. A longer coolant passage might be expected to increase φ and a shorter passage to decrease φ because both the Mach number and the temperature would undergo larger changes in a longer passage than in a shorter one. The magnitudes of these changes were calculated from equation (10) by extending the Mach number and cooling-air temperature-distribution curves an additional 2 inches of span, and then reducing the length of the curves by 2 inches. The results of this calculation are shown in figure 10, where the correction for φ in percent is plotted against the blade span. The rate of change of cooling-air temperature per unit length was assumed to be the same in the additional span as in the original 10-tube-blade span. Four temperature ratios are shown in figure 10. For no heat transfer ($T'_g/T'_{in} = 1.00$), the corrections in φ are small, not exceeding 1 percent over the whole range. The variation over the range of spans increases with the heat-transfer rate so that when the temperature ratio is 3.08, the φ correction varies from -9 percent at a 2-inch span to 17 percent at a 6-inch span.

The other condition that was kept nearly constant during the heat-transfer investigations on the 10-tube blade was the outside heat-transfer coefficient. The heat-transfer rate was varied by changing the temperature of the hot gas. In order to find what change would occur in φ if the heat-transfer rate were varied by changing the outside gas flow, calculations of φ were made for values of H_o half as large and twice as large as the experimental value of 136 Btu per hour per square foot per $^{\circ}F$. The results of this calculation are shown in figure 11 where the percentage correction for φ is plotted against H_o for three temperature ratios. The magnitudes of these corrections are very similar to those produced by changes in blade span, varying from 4 to -1 percent for a temperature ratio of 1.75 and from over 20 to -8 percent for a temperature ratio of 3.08. The largest correction (24 percent) occurred for a temperature ratio of 3.08 and an $H_o = 272$ Btu per hour per square foot per $^{\circ}F$, which is quite high for an outside surface.

Effect of Changes in φ on Blade-Entrance-Pressure Calculations

Pressure calculations are affected by the values chosen for φ when equation (9) is used. In order to find how the range of spans and heat-transfer rates shown in figures 10 and 11 would affect the pressure calculations, values of φ taken from figure 8 for three exit Mach numbers, 1.00, 0.424, and 0.242, were increased and decreased by 25 percent and

the corresponding pressure deviations were calculated. For an increase of 25 percent in φ, the pressure changes were approximately 3, 4, and 5 percent, respectively. When φ was decreased 25 percent, the pressure deviations were 4, 6, and 9 percent, respectively. Thus, over a range of blade spans from 2 to 6 inches and a range of outside heat-transfer coefficients from 68 to 272 Btu per hour per square foot per $^{\circ}F$, the simplified equation (equation (9)) and figure 8 should still give computed pressures within approximately 5 percent of the actual values unless both extreme differences should combine in the same direction, that is, a 6-inch span and a temperature ratio of 3.08, in which case the error might be doubled.

Accuracy of Simplified Flow Equation When Applied to a Rotating Turbine

In order to check the accuracy of the simplified flow equation (equation (11)) as compared to the exact equation (equation (2)), a limited number of examples were obtained wherein blade-entrance static pressures were calculated for the 10-tube blade using equations (11) and (1) and equations (2) and (1). High values of blade-exit Mach number were used in these calculations because the largest discrepancies between the simplified and the exact equations would be expected at high values of M_{ex}.

A change of 25 percent in the parameter φ did not have a serious effect on blade-entrance static pressures calculated for a blade with a stationary passage. Therefore, a value of φ obtained from figure 8 was used for φ_{ω} in equation (11). The results of these calculations show that blade-entrance static pressures calculated from the simplified equation and equation (1) are within 0.50 percent of the values calculated from the exact equation and equation (1).

The conclusions reached from these calculations are: (a) the simplified equation (equation (11)) may be used in place of the exact equation (equation (2)) and thus the tedious numerical integration involved in the solution of equation (2) will be eliminated and (b) no appreciable errors will result if values of φ obtained from figure 8 are used for φ_{ω} in equation (11).

Entrance Effects

In addition to the pressure drop through the test blade, the pressure drop in the entrance section of the test blade was also measured. The curve used for obtaining the entrance loss coefficient in the entrance

section of the 10-tube blade is presented in figure 12. This curve was plotted to determine the magnitude of the losses which occurred in the entrance section of this air-cooled blade. According to reference 4, the maximum value of K which may be expected is 0.50. In this case, however, a value of K = 0.905 was calculated from the experimental line which was determined from equation (17). It is stated in reference 14 that a sudden contraction produces losses that can be completely determined only with the help of experimental data and that the maximum value of K = 0.50 given in reference 4 is at most only an approximation. The value of K = 0.905 obtained for this particular blade-entrance section is therefore not unreasonable. Also, it is evident from experimental data that in many cases the pressure drop through the entrance-blade extension may be as large as that through the test blade.

The conclusion reached in this investigation of entrance sections is that such losses may be quite large, comparable with those inside the blade, and they should be measured in any study of design performance.

RECOMMENDED PROCEDURE FOR CALCULATION OF ROTATING AIR-COOLED-BLADE PRESSURE DROP

In many air-cooled aircraft-engine applications, the cooling air required for the engine would be bled from the engine compressor. The blade-entrance static pressure p_{in} is used in determining the compressor bleed-point. It is desirable to calculate p_{in} with the least amount of effort; consequently, it is suggested that the simplified one-dimensional flow equation (equation (11)) be used in conjunction with equation (1) to calculate an over-all pressure drop through a rotating air-cooled blade in order to eliminate the labor required in the numerical integration of equation (2). In most practical applications of equation (11), the gas-to-blade and blade-to-coolant heat-transfer coefficients, the gas temperature, the required cooling-air weight flow, the angular velocity of the turbine, and the blade geometry will be determined from the turbine- and the compressor-design calculations. The solution of equation (11) for the determination of the blade-entrance static pressure also requires that the blade-exit static pressure p_{ex}, the blade-entrance and -exit cooling-air temperatues T'_{in} and T'_{ex}, and the blade-passage friction coefficient f be known. The blade-exit static pressure is generally assumed to be equal to the static pressure of the combustion gas just downstream of the turbine; this assumption has not been verified experimentally. The value of T'_{in} required for equation (11) is the same as the value of T'_{in} used in determining the required cooling-air weight flow. In many cases this value of T'_{in}, which is used as a first approximation, is usually equal to the total

temperature of the air at the compressor exit. Once a value of T'_{in} is extablished, T'_{ex} may be determined from equations presented in reference 3. It is assumed that the friction coefficient is not affected by rotation as long as the flow through the blade is one-dimensional. Also, it was shown that a change of ±20 percent in f did not have a serious effect on the blade-entrance pressure. It is suggested, therefore, that a value of f be determined from von Kármán's equation (equation (25)) wherein Re is based on the average cooling-air temperature in the blade.

After p_{ex}, T'_{in}, T'_{ex}, and f are determined, the procedure outlined in appendix C is followed except that for a rotating turbine the terms due to rotation are considered. Values for the parameters φ_ω and ψ are determined from figures 8(b) and 9(b), respectively. If the blade under consideration has a span and an outside heat-transfer coefficient different from those of the 10-tube blade, figures 10 and 11 are used to correct the value of φ_ω obtained from figure 8(b). It is not necessary to correct ψ in this manner because over the range of values observed for ψ, the factor $1+b/r_{in}\psi$ changes only 3 percent. Thus, the maximum correction to ψ similar to that required for φ_ω would at most change $1+b/r_{in}\psi$ only by 0.6 percent.

The value obtained for p_{in} in conjunction with the pumping characteristics of the turbine rotor is used to determine the compressor bleed-point. If the air temperature at this bleed-point is significantly different from the value used for the initial value of T'_{in}, it may be necessary to calculate a new value of cooling-air weight flow and blade-entrance static pressure with a new value of T'_{in} based on the compressor bleed-point temperature.

SUMMARY OF RESULTS

The results of an investigation wherein the pressure and temperature changes in the cooling air flowing through two air-cooled turbine-blade configurations were measured experimentally in a static cascade for both isothermal and nonisothermal flows are summarized as follows:

1. When no heat transfer occurred, friction coefficients obtained for the 10-tube blade agreed with values calculated from von Kármán's equation for turbulent flow in smooth round pipes. Friction coefficients obtained for the 13-fin blade were approximately 11 percent below the von Kármán values, but they were in agreement with friction coefficients obtained for small rectangular ducts of large aspect ratios.

2. When heat transfer occurred, the friction coefficients decreased from von Kármán's values as the rate of heat transfer increased. This behavior is observed in turbulent-boundary-layer theory. For a temperature ratio of 3.08, the friction coefficients for the 10-tube blade were approximately 24 percent below the von Kármán values.

3. A friction coefficient determined from von Kármán's equation may be used with the simplified equation for calculations of blade pressure drops if an error of 6 percent in the computed blade-entrance pressure can be tolerated. If greater accuracy is desired, von Kármán's value of f may be corrected for the effect of heat transfer.

2512

4. Simplified one-dimensional flow equations were developed in order to eliminate the labor involved in the numerical integration of the exact one-dimensional flow equation.

5. For air-cooled turbine blades other than the 10-tube blade used in this investigation, that is, blades having spans from 2 to 6 inches, outside heat-transfer coefficients from 68 to 272 Btu per hour per square foot per °F, and ratio of hot-gas to cooling-air temperature from 1.00 to 3.08; the simplified flow equations and the uncorrected values of the equation parameters would still result in computed blade-entrance pressures within approximately 5 percent of the actual values unless both extreme differences occur together, in which case the error could be doubled.

6. The simplified flow-equation parameter developed for static-cascade blades may be used for blades in a rotating turbine.

7. Entrance losses to air-cooled turbine blades may be quite large, compared with the losses inside the blade, and should be measured in any study of design performance.

Lewis Flight Propulsion Laboratory
National Advisory Committee for Aeronautics
Cleveland, Ohio

[redacted]

APPENDIX A - SYMBOLS

The symbols c_p, M, p, Re, T', w, k, γ, μ, and ρ refer to air passing inside blade extensions and blade passage.

The properties c_p, k, μ, and ρ are evaluated on the average of the entrance and exit air temperatures in the passage under consideration.

The following symbols are used in this report:

A flow area, sq ft or sq in.

b length or span, ft or in.

c_p specific heat at constant pressure, Btu/(lb)(°F)

D_h hydraulic diameter, $\frac{\text{4 times free-flow area}}{\text{wetted perimeter}}$, ft or in.

F friction due to sudden contraction, ft-lb/lb fluid

f friction coefficient

f''_w nondimensional measure of velocity gradient at the wall

g standard acceleration of gravity, ft/sec^2

H convection heat-transfer coefficient, Btu/(hr)(sq ft)(°F)

I_A influence coefficient for term involving rate of area change (equation (6))

I_c function of Mach number and ratio of specific heats (equation (18))

I_f influence coefficient for term involving friction (equation (4))

I_R influence coefficient for term involving rotation (equation (5))

I_T influence coefficient for term involving rate of temperature change (equation (3))

K entrance loss coefficient (equation (17))

k thermal conductivity, Btu/(sec)(ft)(°F)

l perimeter, ft or in.

M Mach number relative to blade

[redacted]

Pr Prandtl number, $c_p\mu/k$

p measured static pressure, lb/sq ft abs. (when used with subscript c refers to calculated static pressure)

p' measured total pressure, lb/sq ft abs.

q heat added to coolant, Btu/sec

R gas constant, ft-lb/(lb)($^\circ$R)

Re Reynolds number, $\frac{w\ D_h}{A\mu}$

r distance from turbine center line to any point on turbine blade, ft or in.

T static temperature, $^\circ$R

T' total temperature, $^\circ$R (when used with subscript g refers to air or combustion gas passing over blade)

V velocity relative to blade passage, ft/sec

w air weight flow, lb/sec

x distance along surface, ft or in.

y nondimensional coordinate, $\frac{(r_{in} + b - r)}{b} = \frac{\text{distance from blade exit}}{\text{blade span}}$

γ ratio of specific heats, 1.4

μ viscosity, lb/(ft)(sec)

ρ mass density, lb/cu ft

φ parameter (see equation (10))

ψ parameter (see equation (12))

ω angular velocity, radians/sec

Subscripts:

B blade

ex blade exit

[redacted]

g	combustion gas
I	temperature ratio, $T'_g/T'_{in} = 1.00$ (isothermal)
i	inside of blade
in	blade entrance
m	mean value
o	outside of blade
vK	von Kármán
w	wall
x	distance along surface
1	entrance plenum chamber
2	exit plenum chamber
3	entrance-blade extension
4	exit-blade extension
ω	rotating turbine
∞	main stream

APPENDIX B

DERIVATION OF SIMPLIFIED ONE-DIMENSIONAL FLOW EQUATION

The momentum equation (equation (9) in reference 3) is

$$\frac{dM^2}{dy} = \frac{I_T}{T'}\frac{dT'}{dy} - I_f\left[\frac{4fb}{D_h} - \frac{I_R}{T'}\frac{2\omega^2 r_{in} b}{gR}\left(1 + \frac{b}{r_{in}} - y\frac{b}{r_{in}}\right)\right] + \frac{I_A}{A}\frac{dA}{dy} \quad (2)$$

where

$$I_T = \frac{M^2\,(1 + \gamma M^2)\left(1 + \frac{\gamma-1}{2}M^2\right)}{1 - M^2} \quad (3)$$

$$I_f = \frac{\gamma M^4\,\left(1 + \frac{\gamma-1}{2}M^2\right)}{1 - M^2} \quad (4)$$

$$I_R = \frac{1 + \frac{\gamma-1}{2}M^2}{\gamma M^2} \quad (5)$$

$$I_A = -\frac{2M^2\,\left(1 + \frac{\gamma-1}{2}M^2\right)}{1 - M^2} \quad (6)$$

If the rotational term and the term for varying blade-passage area are eliminated and equation (2) is divided through by I_f,

$$\frac{1}{I_f}\,dM^2 = \frac{I_T}{I_f}\frac{1}{T'}\cdot dT' - \frac{4fb}{D_h}\,dy \quad (B1)$$

Substitution of equations (3) and (4) in equation (B1) yields

$$\frac{(1 - M^2)\,dM^2}{\gamma M^4\,\left(1 + \frac{\gamma-1}{2}M^2\right)} = \frac{(1 + \gamma M^2)}{\gamma M^2}\,\frac{dT'}{T'} - \frac{4fbdy}{D_h} \quad (B2)$$

or

$$\frac{(1 - M^2)\,dM^2}{M^4\,\left(1 + \frac{\gamma-1}{2}M^2\right)} = \frac{1}{M^2}\frac{dT'}{T'} + \frac{\gamma dT'}{T'} - \frac{4\gamma fbdy}{D_h} \quad (B3)$$

[redacted]

Equation (B3) is integrated with the following limits:

M; from M_{ex} to M_{in}

T; from T'_{ex} to T'_{in}

y; from 0 to 1.0

For no heat transfer, equation (B3) reduces to

$$\int_{M_{ex}}^{M_{in}} \frac{(1 - M^2)\, dM^2}{M^4 \left(1 + \frac{\gamma-1}{2} M^2\right)} = -\int_0^{1.0} \frac{4\gamma f b\, dy}{D_h} \tag{B4}$$

where integration by partial fraction yields

$$\int_{M_{ex}}^{M_{in}} \frac{(1 - M^2)\, dM^2}{M^4 \left(1 + \frac{\gamma-1}{2} M^2\right)} = \frac{1}{M_{ex}^2} - \frac{1}{M_{in}^2} + 1.2 \ln \frac{1 + 0.2\, M_{in}^2}{1 + 0.2\, M_{ex}^2} \cdot \frac{M_{ex}^2}{M_{in}^2} \tag{B5}$$

and

$$-\int_0^{1.0} \frac{4\gamma f b\, dy}{D_h} = -\frac{4\gamma f b}{D_h} \tag{B6}$$

Therefore, equation (B4) may be integrated to

$$\frac{1}{M_{in}^2} = \frac{1}{M_{ex}^2} + 1.2 \ln \frac{M_{ex}^2}{M_{in}^2} \frac{1 + 0.2\, M_{in}^2}{1 + 0.2\, M_{ex}^2} + \frac{4\gamma f b}{D_h} \tag{7}$$

for the no-heat-transfer case.

For the case of heat transfer, equation (B3) becomes

$$\int_{M_{ex}}^{M_{in}} \frac{(1 - M^2)\, dM^2}{M^4 \left(1 + \frac{\gamma-1}{2} M^2\right)} = \int_{T'_{ex} M_{ex}}^{T'_{in} M_{in}} \frac{dT'}{M^2 T'} + \int_{T'_{ex}}^{T'_{in}} \frac{\gamma\, dT'}{T'} - \int_0^{1.0} \frac{4\gamma f b\, dy}{D_h} \tag{B7}$$

By exact integration

$$\int_{T'_{ex}}^{T'_{in}} \frac{\gamma dT'}{T'} = \gamma \ln \frac{T'_{in}}{T'_{ex}} \tag{B8}$$

The term $\int_{T'_{ex}M_{ex}}^{T'_{in}M_{in}} \frac{dT'}{M^2T'}$ cannot be integrated directly. It has been determined from experimental evidence, however, that the true mean of $\frac{1}{M^2T'}$ equals the arithmetic mean of $\frac{1}{M^2T'}$ within ±12 percent. Therefore, the parameter φ is introduced in order to evaluate the integral $\int \frac{dT'}{M^2T'}$. The parameter φ, a pure number, is a ratio of the arithmetic and the true mean of $\frac{1}{M^2T'}$ and is defined as

$$\varphi = - \frac{\frac{1}{2}\left[\left(\frac{1}{M^2T'}\right)_{in} + \left(\frac{1}{M^2T'}\right)_{ex}\right]}{\frac{1}{T'_{ex} - T'_{in}} \int_{T'_{ex}}^{T'_{in}} \frac{dT'}{M^2T'}} \tag{10}$$

Therefore, for the heat-transfer case equation (B7) becomes

$$\frac{1}{M_{in}^2} = \frac{1}{M_{ex}^2} + 1.2 \ln \frac{M_{ex}^2}{M_{in}^2} \frac{1+0.2\,M_{in}^2}{1+0.2\,M_{ex}^2} + \frac{4\gamma f b}{D_h} + \gamma \ln \frac{T'_{ex}}{T'_{in}} + \frac{(T'_{ex} - T'_{in})}{\varphi} \left(\frac{1}{M^2T'}\right)_m \tag{9}$$

Equation (9) is a simplified one-dimensional flow equation for an air-cooled turbine blade having a stationary passage and a constant flow area. For a rotating turbine, the blade coolant flow area is assumed to be constant and the values of I_T, I_f, and I_R may be substituted in equation (2). Thus, because of rotation equation (B3) will contain the additional term

$$\frac{2\omega^2 r_{in} b}{gR} \frac{\left(1 + \frac{\gamma-1}{2} M^2\right)}{M^2T'} \left(1 + \frac{b}{r_{in}} - \frac{b}{r_{in}} y\right) dy \tag{B9}$$

For subsonic flow, $M^2 < 1.00$, the term $\left(1 + \frac{\gamma-1}{2} M^2\right)$ does not have a

large range of values through the blade. Therefore, when this term is integrated through the blade passage, a mean constant value can be used for $\left(1 + \frac{\gamma-1}{2} M^2\right)$ without much error. This mean value is

$$\left(1 + \frac{\gamma-1}{2} M^2\right)_m = \frac{1}{2}\left[\left(1 + \frac{\gamma-1}{2} M_{in}^2\right) + \left(1 + \frac{\gamma-1}{2} M_{ex}^2\right)\right] \tag{B10}$$

Integration of equation (B9) yields

$$\frac{2\omega^2 r_{in} b}{gR}\left(1 + \frac{\gamma-1}{2} M^2\right)_m \int_0^{1.0} \frac{\left(1 + \frac{b}{r_{in}} - \frac{b}{r_{in}} y\right)dy}{M^2 T'} \tag{B11}$$

Integration of the integral (B11) gives

$$\left(1 + \frac{b}{r_{in}}\right)\int_0^{1.0} \frac{dy}{M^2 T'} - \frac{b}{r_{in}}\int_0^{1.0} \frac{dy}{M^2 T'} + \frac{b}{r_{in}}\int_0^{1.0}\int_0^{y} \frac{dy}{M^2 T'}\,dy \tag{B12}$$

The integral $\int \frac{dT'}{M^2 T'}$ in equation (10) may be written in the form $\frac{dT'}{dy}\int \frac{dy}{M^2 T'}$ because the cooling-air temperature distribution curve is assumed to be linear in this investigation. When $\frac{dT'}{dy}\int \frac{dy}{M^2 T'}$ is substituted in equation (10), the denominator becomes $\int_0^{1.0} \frac{dy}{M^2 T'}$ because $-dT'/dy = T'_{ex} - T'_{in}$. Thus, equation (10) becomes

$$\varphi = \frac{\left(\frac{1}{M^2 T'}\right)_m}{\int_0^{1.0} \frac{dy}{M^2 T'}} \tag{B13}$$

If equation (B13) is substituted into (B12) wherein φ becomes φ_ω for a rotating turbine, the result is

$$\frac{1}{\varphi_\omega}\left(\frac{1}{M^2 T'}\right)_m \left[1 + \frac{b}{r_{in}} \frac{\int_0^{1.0}\int_0^{y} \frac{dy}{M^2 T'}\,dy}{\int_0^{1.0} \frac{dy}{M^2 T'}}\right] \tag{B14}$$

2512

or

$$\frac{1}{\varphi_\omega}\left(\frac{1}{M^2T'}\right)_m\left[1+\frac{b}{r_{in}}\psi\right] \tag{B15}$$

if the parameter ψ in equation (B15) is defined as

$$\psi=\frac{\int_0^{1.0}\int_0^{y}\frac{dy}{M^2T'}\,dy}{\int_0^{1.0}\frac{dy}{M^2T'}} \tag{12}$$

Then, for the case of a rotating turbine the simplified one-dimensional flow equation may be written

$$\frac{1}{M_{in}^2}=\frac{1}{M_{ex}^2}+1.2\ln\frac{M_{ex}^2}{M_{in}^2}\frac{1+0.2\,M_{in}^2}{1+0.2\,M_{ex}^2}+\frac{4\gamma fb}{D_h}+\gamma\ln\frac{T'_{ex}}{T'_{in}}+$$

$$\frac{T'_{ex}-T'_{in}}{\varphi_\omega}\left(\frac{1}{M^2T'}\right)_m-\frac{2\omega^2r_{in}b}{gR}\left(1+\frac{\gamma-1}{2}M^2\right)_m\frac{1}{\varphi_\omega}\left(\frac{1}{M^2T'}\right)_m\left(1+\frac{b}{r_{in}}\psi\right) \tag{11}$$

[redacted]

APPENDIX C

SAMPLE CALCULATION OF BLADE-ENTRANCE STATIC PRESSURE FOR 10-TUBE BLADE WITH SIMPLIFIED EQUATION ($T'_g/T'_{in} > 1.00$)

The blade-entrance static pressure for a typical heat-transfer case will be calculated using equations (9) and (1). The data required for this numerical example are as follows:

A_B 0.00126, sq ft

b_B 0.327, ft

$D_{h,B}$ 0.008615, ft

f 0.00565

p_{ex} 1145, lb/sq ft abs

R 53.3, (ft-lb)/(lb)($^\circ$F)

T'_g 1465°, R

T'_{in} 459°, R

T'_{ex} 659°, R

w 0.03932, lb/sec

γ 1.4

μ_B 132.3×10^{-7}, lb/(sec)(ft)

The computations are as follows:

Calculate M_{ex} from equation (18) and table I of reference 3.

$$M_{ex} = 0.7236$$

Now, it is desired to calculate M_{in} and p_{in} from the simplified equation (9) and equation (1).

$$\frac{1}{M_{in}^2} = \frac{1}{M_{ex}^2} + 1.2 \ln \frac{M_{ex}^2}{M_{in}^2} \frac{1+0.2\,M_{in}^2}{1+0.2\,M_{ex}^2} + \frac{4\gamma f b}{D_h} + \gamma \ln \frac{T'_{ex}}{T'_{in}} + \frac{(T'_{ex}-T'_{in})}{\varphi} \left(\frac{1}{M^2T'}\right)_m \quad (9)$$

The following quantities required in equation (9) are calculated from known experimental or calculated values.

$$\frac{1}{M_{ex}^2} = 1.910$$

$$\frac{4\gamma f b}{D_h} = 1.199$$

$$\gamma \ln \frac{T'_{ex}}{T'_{in}} = 0.506$$

$$(T'_{ex} - T'_{in}) = 200$$

It is now necessary to assume values for $1.2 \ln \frac{M_{ex}^2}{M_{in}^2} \frac{1+0.2\,M_{in}^2}{1+0.2\,M_{ex}^2}$ and $(T'_{ex} - T'_{in}) \left(\frac{1}{M^2T'}\right)_m$ so that a starting value for $\frac{1}{M_{in}^2}$ can be determined. It is suggested that a value of 1.00 be assumed for $1.2 \ln \frac{M_{ex}^2}{M_{in}^2} \frac{1+0.2\,M_{in}^2}{1+0.2\,M_{ex}^2}$ for a starting value. The following values are suggested for $(T'_{ex} - T'_{in}) \left(\frac{1}{M^2T'}\right)_m$.

If

$(T'_{ex} - T'_{in}) \leq 150$	assume 1.00
$150 \leq (T'_{ex} - T'_{in}) \leq 200$	assume 2.00
$210 \leq (T'_{ex} - T'_{in}) \leq 250$	assume 3.00
$260 \leq (T'_{ex} - T'_{in}) \leq 300$	assume 5.00
$(T'_{ex} - T'_{in}) > 300$	assume 10.00

By use of the known and the suggested values for the various terms in equation (8), a starting value for $\frac{1}{M_{in}^2}$ can be obtained.

[redacted]

$$\frac{1}{M_{in}^2} = 1.910 + 1.000 + 1.199 + 0.506 + 2.000 \quad \text{(see equation (9))}$$

$$\frac{1}{M_{in}^2} = 6.615$$

from which

$$M_{in} = 0.3889$$

Now, with $M_{in} = 0.3889$ and $M_{ex} = 0.7236$

$$1.2 \ln \frac{M_{ex}^2}{M_{in}^2} \frac{1 + 0.2 M_{in}^2}{1 + 0.2 M_{ex}^2} = 1.405$$

and by using the arithmetic mean of $\left(\frac{1}{M^2T'}\right)$

$$(T'_{ex} - T'_{in}) \left(\frac{1}{M^2T'}\right)_m = (T'_{ex} - T'_{in}) \left[\frac{\left(\frac{1}{M_{in}^2 T'_{in}} + \frac{1}{M_{ex}^2 T'_{ex}}\right)}{2}\right] = 1.731$$

The true value of $(T'_{ex}-T'_{in}) \left(\frac{1}{M^2T'}\right)$ can be obtained by determining φ from figure 8(b) as 1.119. Thus, the true value is

$$\frac{1.731}{1.119} = 1.547$$

Substitution of these new values in equation (9) gives

$$\frac{1}{M_{in}^2} = 1.910 + 1.405 + 1.199 + 0.506 + 1.547$$

$$\frac{1}{M_{in}^2} = 6.567$$

This results in an error of 0.048 between the starting value and final value of $\frac{1}{M_{in}^2}$. If $\frac{1}{M_{in}^2} = 6.567$ is used as the new starting value and the same procedure is followed,

$$\frac{1}{M_{in}^2} = 6.550$$

[redacted]

There is an error of 0.017 between starting and final values of $\frac{1}{M_{in}^2}$. Now, $\frac{1}{M_{in}^2} = 6.550$ is used as a starting value and the resulting final value is

$$\frac{1}{M_{in}^2} = 6.543$$

with an error of 0.007 between the starting and final values of $\frac{1}{M_{in}^2}$. Because this error is insignificant, $\frac{1}{M_{in}^2} = 6.543$ will be used. Therefore,

$$M_{in} = 0.3908$$

The blade-entrance static pressure is then calculated from equation (1)

$$p_{in,c} = p_{ex} \frac{A_{ex}}{A_{in}} \frac{M_{ex}}{M_{in}} \sqrt{\frac{T'_{in}}{T'_{ex}} \left(\frac{1 + \frac{\gamma-1}{2} M_{ex}^2}{1 + \frac{\gamma-1}{2} M_{in}^2} \right)}$$

$$= (1145) \left(\frac{0.00126}{0.00126} \right) \left(\frac{0.7236}{0.3908} \right) \sqrt{\left(\frac{459}{659} \right) \left(\frac{1+0.2(0.7236)^2}{1+0.2(0.3908)^2} \right)}$$

$$= 1832 \text{ lb/sq ft abs}$$

The observed value of p_{in} is 1835 lb/sq ft abs

APPENDIX D

THEORETICAL EFFECT OF HEAT TRANSFER ON FRICTION COEFFICIENT

It is shown in reference 15 that in the case of a laminar boundary layer the friction coefficient is

$$f = \frac{2f''_w}{\sqrt{Re_{x,w}}} \frac{T_\infty}{T_w} \tag{D1}$$

where f''_w is a nondimensional measure of the velocity gradient at the wall, T_∞ is the stream temperature, and T_w is the wall temperature.

In reference 14, the Reynolds number of equation (D1) is defined as

$$Re_{x,w} = \frac{V_\infty \rho_w x}{\mu_w} \tag{D2}$$

whereas in the present investigation

$$Re_{x,\infty} = \frac{V_\infty \rho_\infty x}{\mu_\infty} \tag{D3}$$

Thus, for this investigation equation (D1) becomes

$$f = \frac{2f''_w}{\sqrt{Re_{x,\infty}}} \frac{T_\infty}{T_w} \sqrt{\frac{\rho_\infty}{\rho_w} \frac{\mu_w}{\mu_\infty}} \tag{D4}$$

When the following equalities are used:

$$\frac{\mu_\infty}{\mu_w} \cong \left(\frac{T_\infty}{T_w}\right)^{0.7} \tag{D5}$$

and

$$\frac{\rho_\infty}{\rho_w} = \left(\frac{T_w}{T_\infty}\right) \tag{D6}$$

Equation (D4) becomes

[redacted]

$$f = \frac{2f''_w}{\sqrt{Re_{x,\infty}}} \left(\frac{T_\infty}{T_w}\right)^{0.15} \tag{D7}$$

If the temperature ratio is 1.00, equation (D7) becomes

$$f_I = \frac{2f''_{w,I}}{\sqrt{Re_{x,\infty}}} \tag{D8}$$

so that

$$\frac{f}{f_I} = \frac{f''_w}{f''_{w,I}} \left(\frac{T_\infty}{T_w}\right)^{0.15} \tag{D9}$$

If the boundary layer becomes turbulent, then f will vary as $Re^{-0.2}$ instead of $Re^{-0.5}$ and thus for the turbulent case equation (D9) becomes

$$\frac{f}{f_I} = \frac{f''_w}{f''_{w,I}} \left(\frac{T_\infty}{T_w}\right)^{0.66} \tag{D10}$$

Values of f''_w, given in table II of reference 15 for an Euler number of 1.00, appear in the first two columns of the following table. The values appearing in the remaining columns are calculated according to the indicated headings.

1	2	3	4	5	6
$\frac{T_\infty}{T_w}$	f''_w	$\left(\frac{T_\infty}{T_w}\right)^{0.15}$	$\left(\frac{T_\infty}{T_w}\right)^{0.66}$	$\frac{f}{f_I}$ (laminar) Equation (D9)	$\frac{f}{f_I}$ (turbulent) Equation (D10)
2	0.900	1.110	1.580	0.810	1.161
1	1.233	1	1	1	1
1/2	1.800	.901	.633	1.315	.924
1/4	2.784	.812	.401	1.833	.905

[redacted]

The values of f''_w shown in column 2 are for the laminar case, not the turbulent one. The relative values of f''_w are not known exactly for the turbulent boundary layer, but it is known that the effects of changing the pressure gradient and the wall temperature are proportionately less for a turbulent boundary layer than for a laminar one. For example, the effect of a variable wall temperature on the heat-transfer coefficient (analogous to f''_w according to Reynolds) has been calculated for a laminar boundary layer in reference 16, and for a turbulent boundary layer in reference 17. For the same wall-temperature variation, the ratio H/H_I is consistently smaller for the turbulent layer. Therefore, the relative increase of f''_w should be smaller and the relative decrease of f/f_I in column 6 should be larger than that shown. In conclusion then, the trend shown in column 6 should be correct but the magnitude is probably too small.

REFERENCES

1. Ellerbrock, Herman H., Jr.: Preliminary Analysis of Problem of Determining Experimental Performance of Air-Cooled Turbine. II - Methods for Determining Cooling-Air-Flow Characteristics. NACA RM E50A06, 1950.

2. Shapiro, Ascher H., and Hawthorne, W. R.: The Mechanics and Thermodynamics of Steady One-Dimensional Gas Flow. Jour. Appl. Mech., vol. 14, no. 4, Dec. 1947, pp. A317-A336.

3. Brown, W. Byron, and Rossbach, Richard J.: Numerical Solution of Equations for One-Dimensional Gas Flow in Rotating Coolant Passages. NACA RM E50E04, 1950.

4. McAdams, William H.: Heat Transmission. McGraw-Hill Book Co., Inc., 2d ed., 1942.

5. von Kármán, Th.: Turbulence and Skin Friction. Jour. Aero. Sci., vol. 1, no. 1, Jan. 1934, pp. 1-20.

6. Lowdermilk, Warren H., and Grele, Milton D.: Heat Transfer from High-Temperature Surfaces to Fluids. II - Correlation of Heat-Transfer and Friction Data for Air Flowing in Inconel Tube with Rounded Entrance. NACA RM E8L03, 1949.

7. Gallagher, James J., and Habel, Louis W.: Experimental Data Concerning the Effect of High Heat-Input Rates on the Pressure Drop Through Radiator Tubes. NACA RM L8F18, 1948.

8. Washington, Lawrence, and Marks, William M.: Heat Transfer and Pressure Drop in Rectangular Air Passages. Ind. and Eng. Chem., vol. 29, no. 3, March 1937, pp. 337-345.

9. Ellerbrock, Herman H., Jr., and Stepka, Francis S.: Experimental Investigation of Air-Cooled Turbine Blades in Turbojet Engine. I - Rotor Blades with 10 Tubes in Cooling-Air Passages. NACA RM E50I04, 1950.

10. Stepka, Francis S., and Hickel, Robert O.: Experimental Investigation of Air-Cooled Turbine Blades in Turbojet Engine. IX - Evaluation of the Durability of Noncritical Rotor Blades in Engine Operation. NACA RM E51J10, 1951.

11. Esgar, Jack B., and Clure, John L.: Experimental Investigation of Air-Cooled Turbine Blades in Turbojet Engine. X - Endurance Evaluation of Several Tube-Filled Rotor Blades. NACA RM E52B13, 1952.

12. Shapiro, Ascher H., and Smith, R. Douglas: Friction Coefficients in the Inlet Length of Smooth Round Tubes. NACA TN 1785, 1948.

13. Humble, Leroy V., Lowdermilk, Warren H., and Desmon, Leland G.: Measurements of Average Heat-Transfer and Friction Coefficients for Subsonic Flow of Air in Smooth Tubes at High Surface and Fluid Temperatures. NACA Rep. 1020, 1951. (Supersedes NACA RM's E7L31, E8L03, E50E23, and E50H23.)

14. Dodge, Russell A., and Thompson, Milton J.: Fluid Mechanics. McGraw-Hill Book Co., Inc., 1st ed., 1937.

15. Brown, W. Byron, and Donoughe, Patrick L.: Tables of Exact Boundary-Layer-Solutions When the Wall is Porous and Fluid Properties are Variable. NACA TN 2479, 1951.

16. Levy, S.: Heat Transfer to Constant Property Laminar Boundary Layer Flows with Power Function Free Stream Velocity and Wall Temperature Variation. Rep. 5, Ser. 41, Inst. Eng. Res., Univ. California (Berkeley), July 25, 1951. (AMC Contract No. 33(038)-12941.)

17. Rubesin, Morris W.: The Effect of an Arbitrary Surface-Temperature Variation Along a Flat Plate on the Convective Heat Transfer in an Incompressible Turbulent Boundary Layer. NACA TN 2345, 1951.

TABLE I - SUMMARY OF OPERATING CONDITIONS

Blade	Number of runs	Type of investigation	Approximate gas temperature (°F)	Approximate cooling-air temperature (°F)	Cooling-air weight flow per blade (lb/sec)
10-Tube	25	No heat transfer	100	100	0.006-0.051
	8	Heat transfer	300	-30	.011- .057
	9	Reverse heat transfer	100	500	.012- .037
	6	Reverse heat transfer	100	300	.014- .048
	10	No heat transfer	100	100	.012- .051
	8	Heat transfer	1000	-30	.018- .049
	10	No heat transfer	100	100	.010- .053
	8	Heat transfer	1000	-30	.016- .052
	10	Heat transfer	600	-30	.017- .053
13 Fin	24	No heat transfer	85	85	0.008-0.063

[redacted]

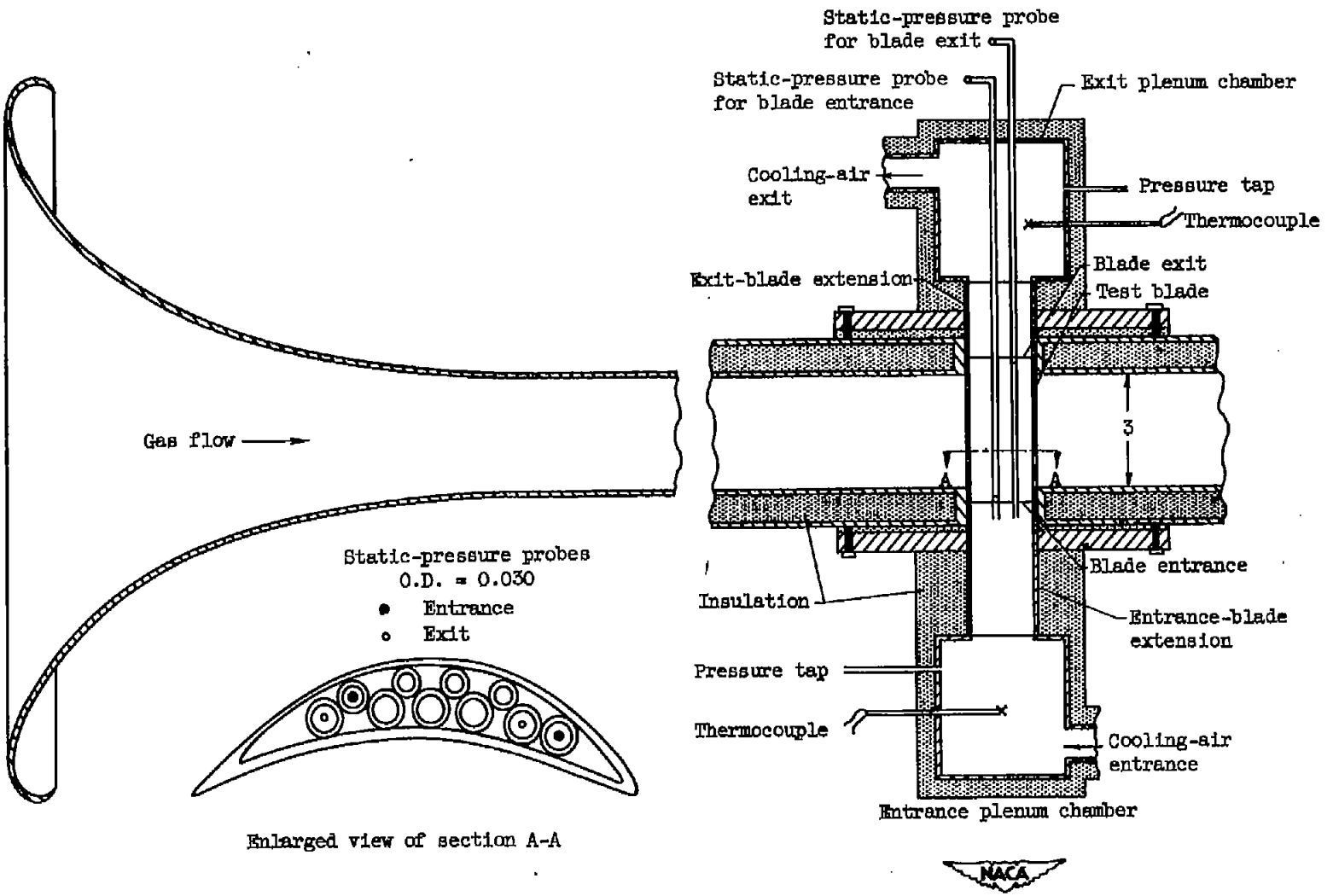

Figure 1. - Sectional view of blade test section showing instrumentation. (All dimensions in inches.)

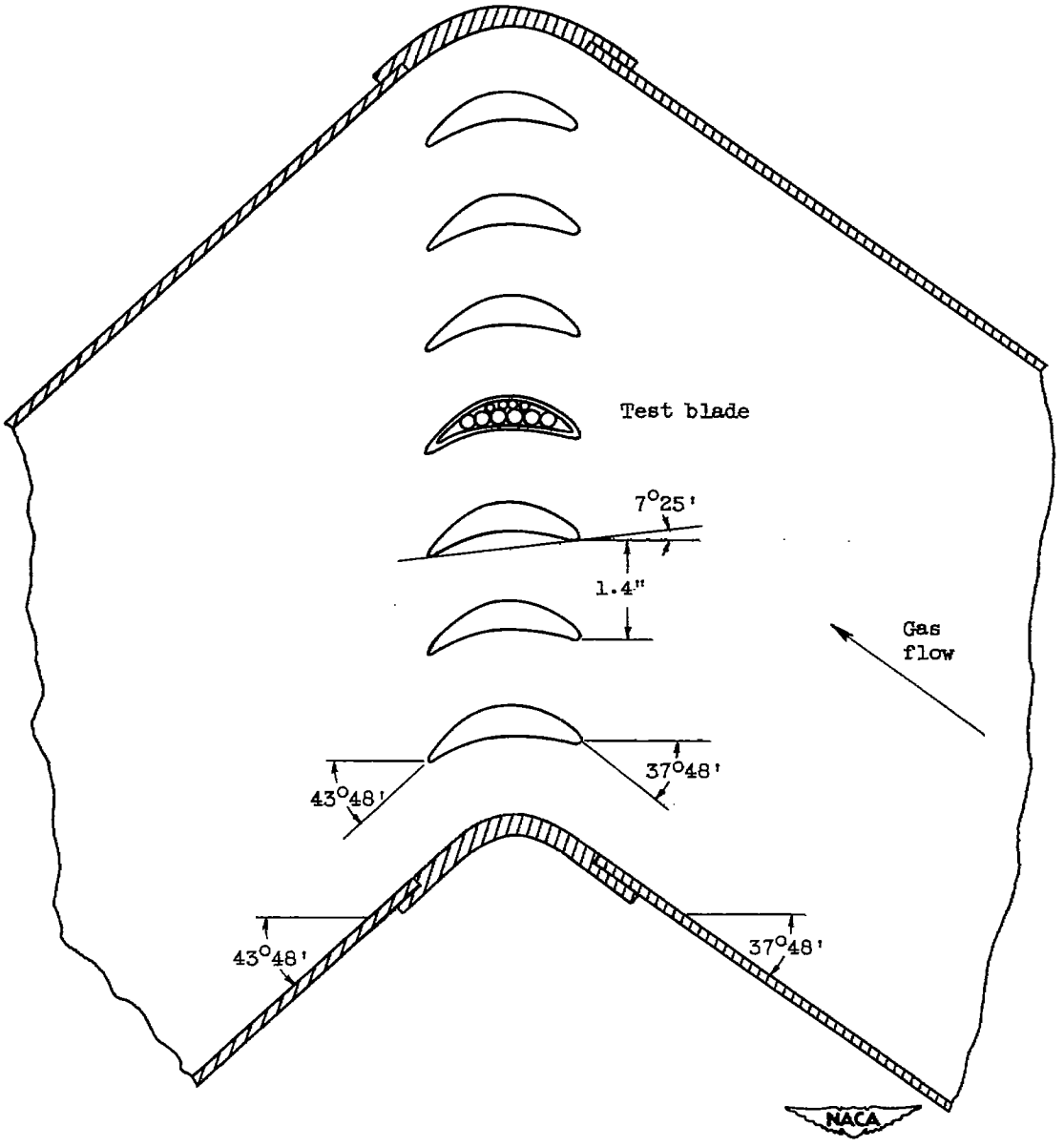

Figure 2. - Cascade geometry.

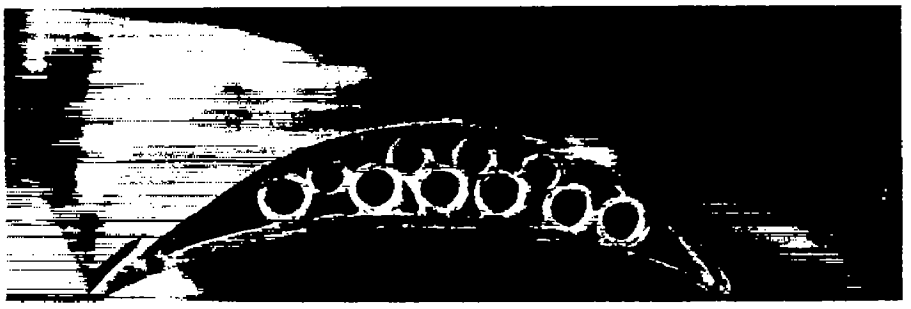

10-tube blade

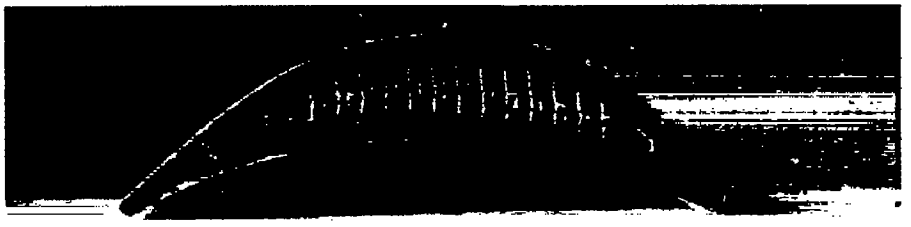

13-fin blade

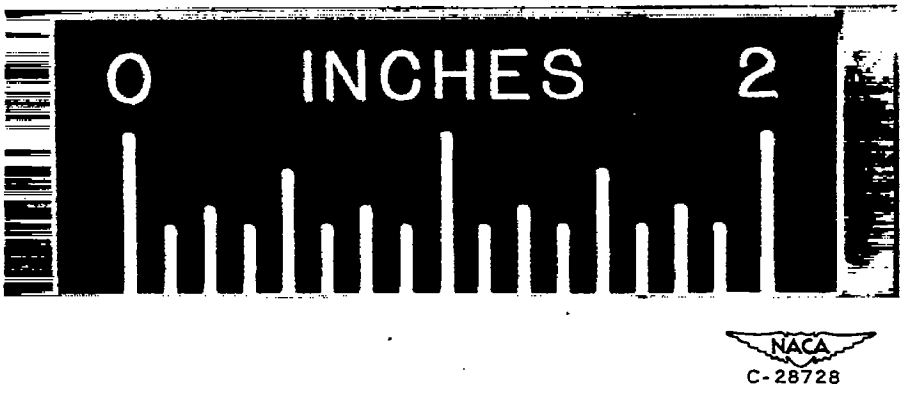

Figure 3. - Cross-sectional view of air-cooled turbine-blade configurations used in this investigation.

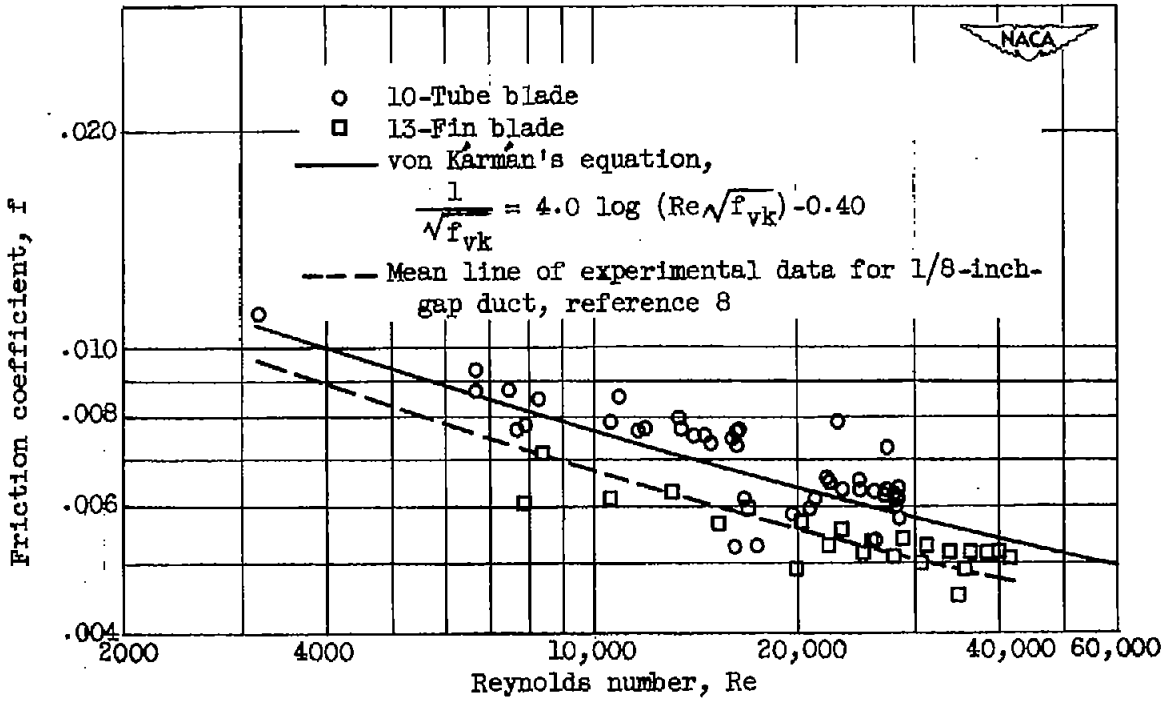

Figure 4. - Comparison of variation of friction coefficient with Reynolds number for 10-tube and 13-fin blades with von Kármán's equation for flow in smooth pipes ($T'_g/T'_{in} = 1.00$).

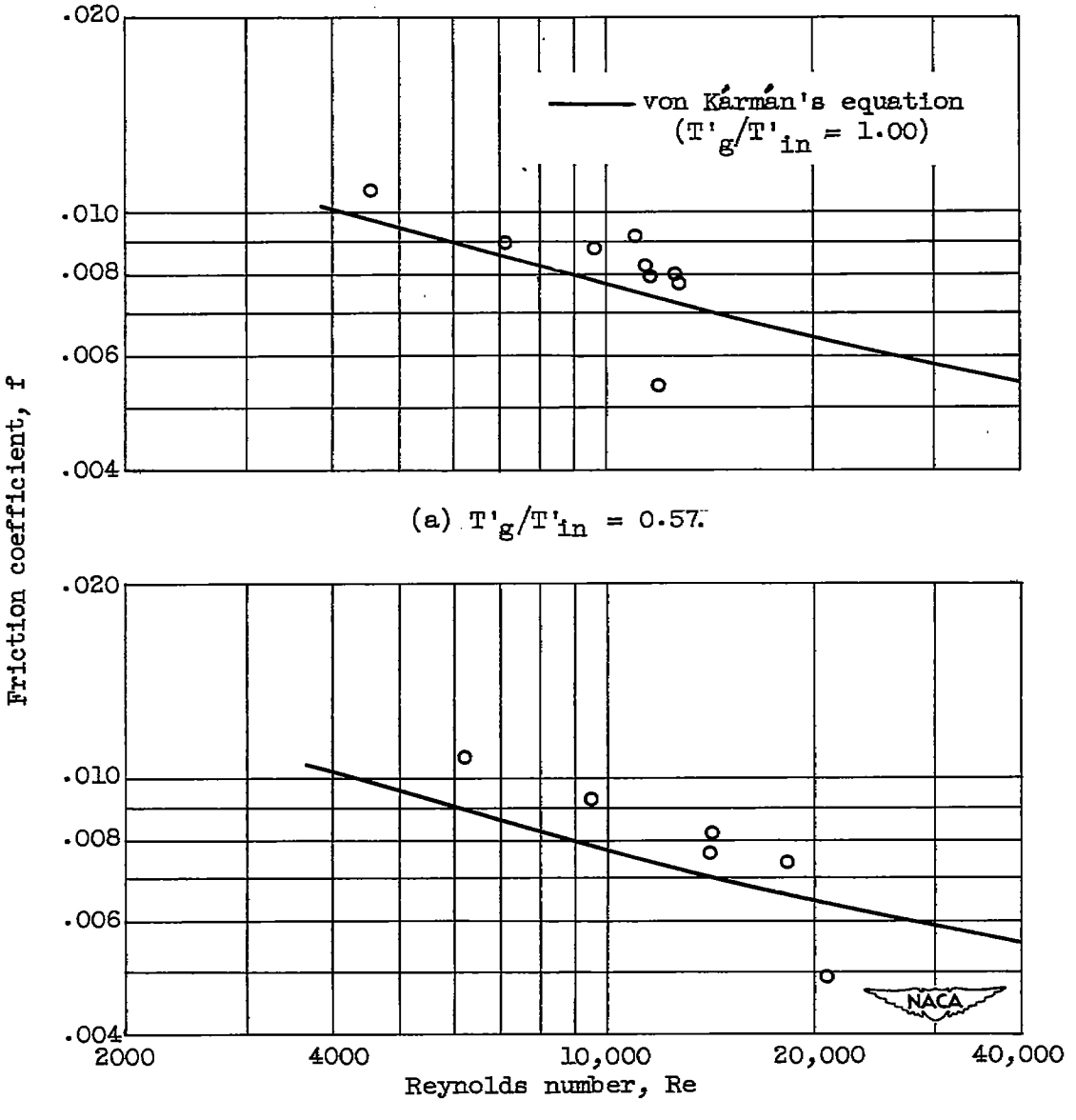

(a) $T'_g/T'_{in} = 0.57$.

(b) $T'_g/T'_{in} = 0.73$.

Figure 5. - Effect of heat transfer on friction coefficient for 10-tube blade.

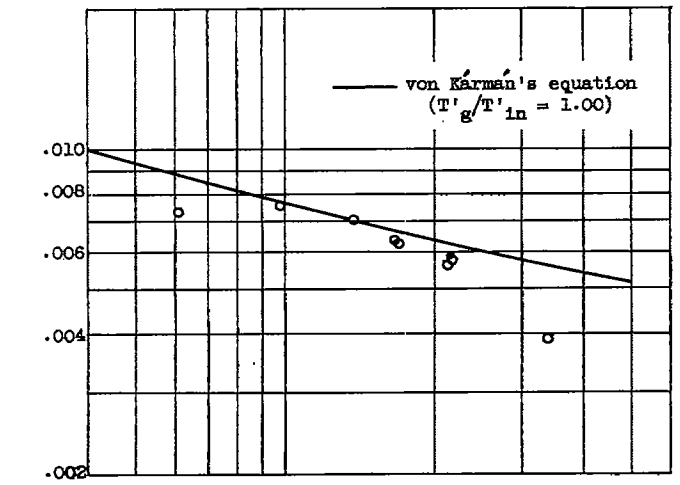

(c) $T'_g/T'_{in} = 1.75$.

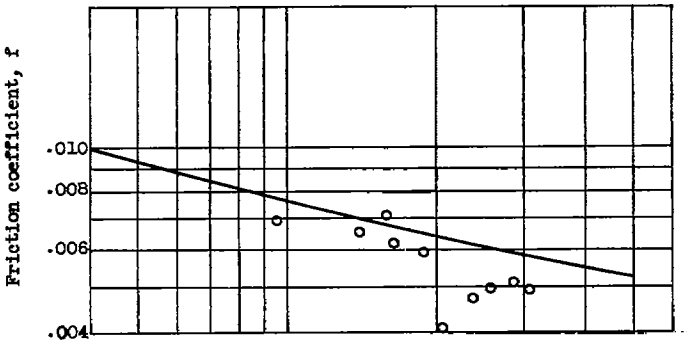

(d) $T'_g/T'_{in} = 2.37$.

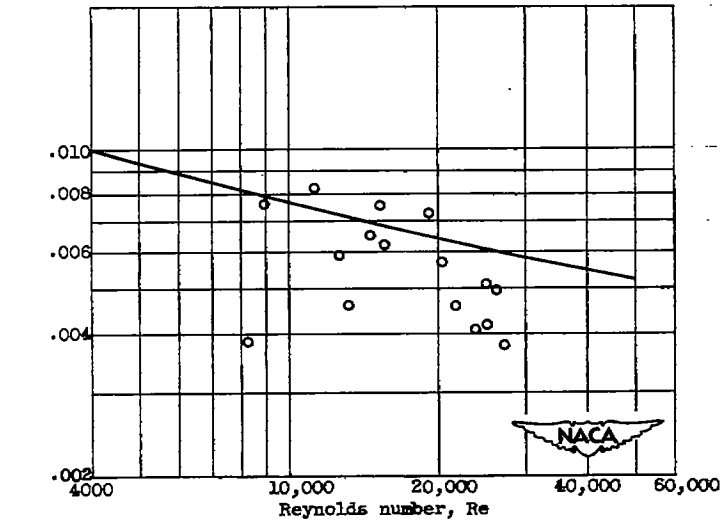

(e) $T'_g/T'_{in} = 3.08$.

Figure 5. - Concluded. Effect of heat transfer on friction coefficient for 10-tube blade.

[redacted]

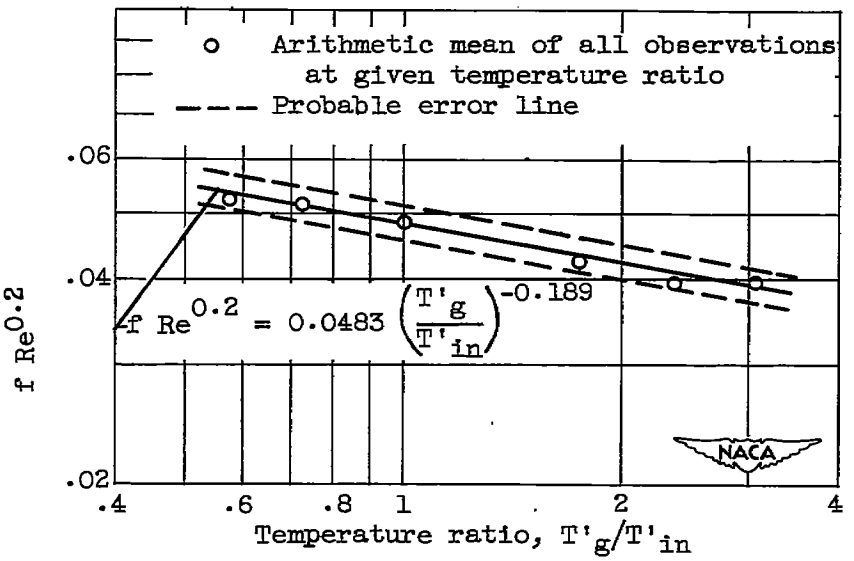

Figure 6. - Effect of temperature ratio on friction coefficient. Outside heat-transfer coefficient, H_o, 136 Btu per hour per square foot per °F.

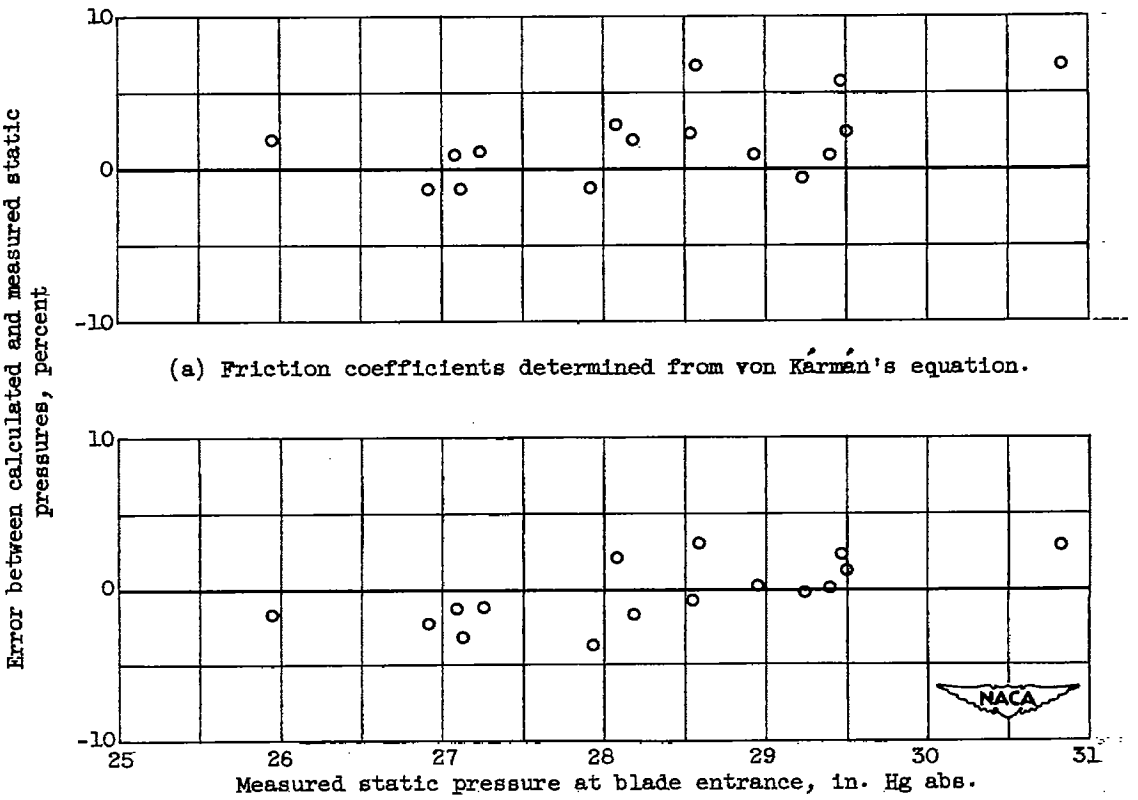

(a) Friction coefficients determined from von Kármán's equation.

(b) Friction coefficients determined from von Kármán's equation and corrected for effect of heat transfer.

Figure 7. - Variation between calculated and measured blade-entrance static pressures for 10-tube blade when theoretical friction coefficients are used in simplified flow equation. (T'_g/T'_{in} = 3.08.)

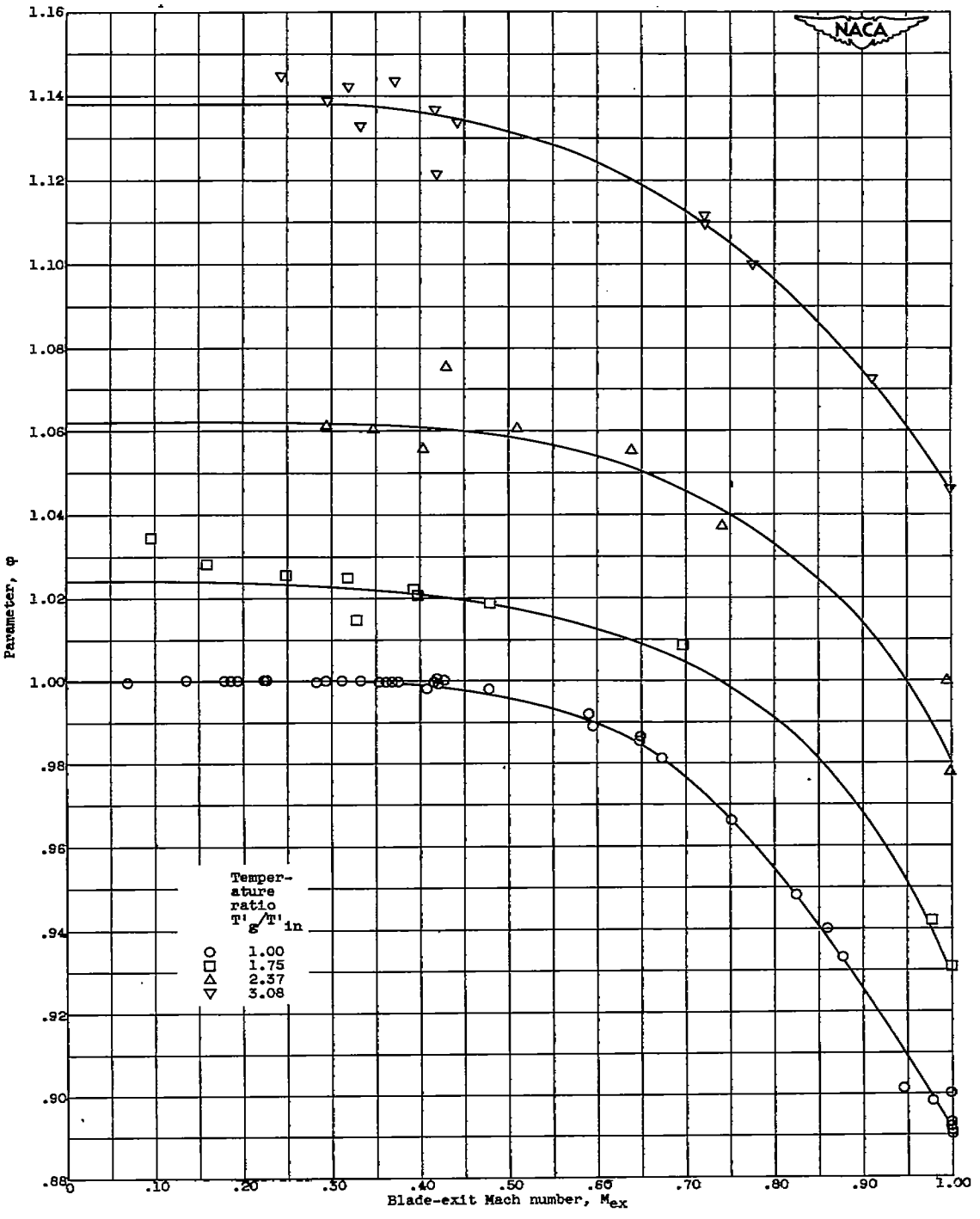

(a) Various temperature ratios.

Figure 8. - Chart used for evaluating $\int_0^{1.0} \frac{dy}{M^2 T'}$.

[redacted]

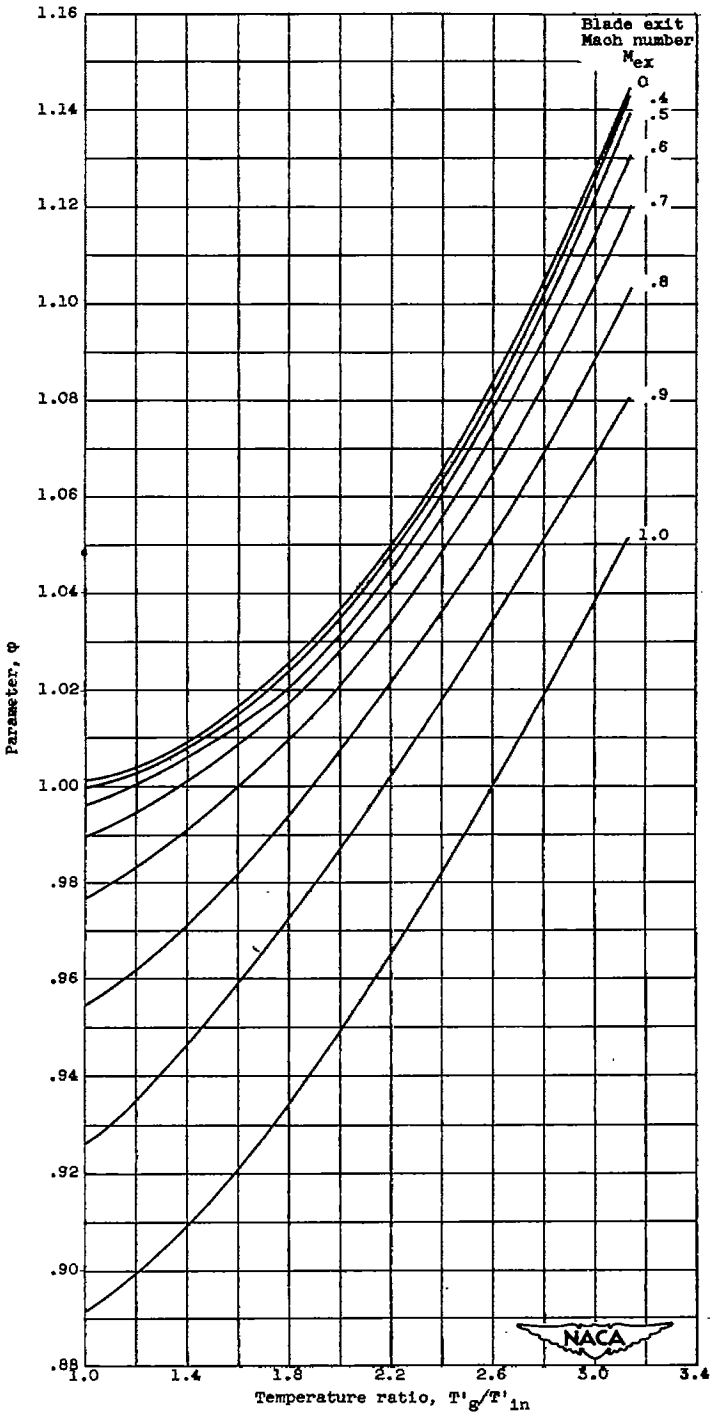

(b) Various Mach numbers.

Figure 8. - Concluded. Chart used for evaluating $\int_0^{1.0} \frac{dy}{M^2 T'}$.

[redacted]

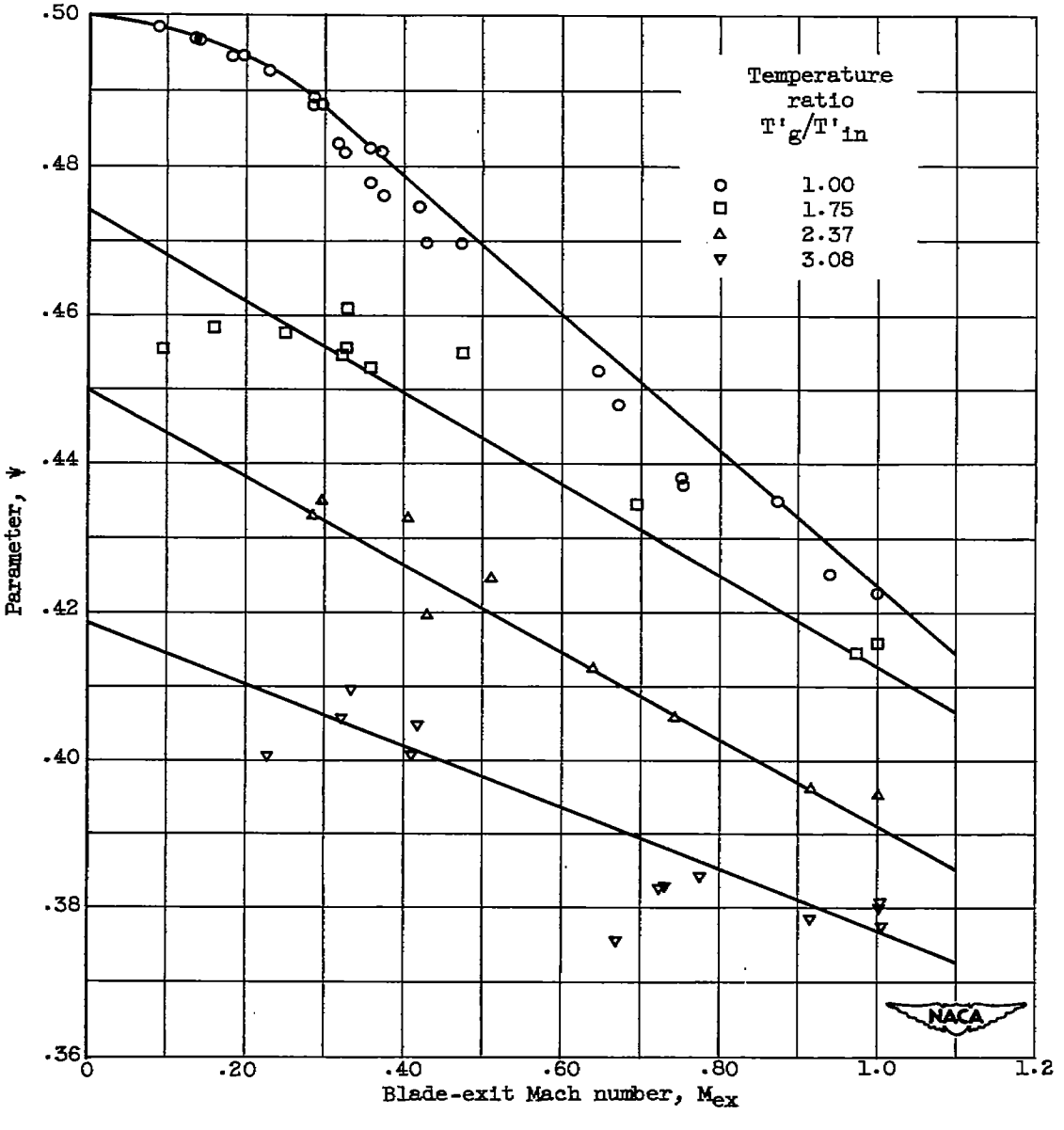

(a) Various temperature ratios.

Figure 9. - Chart used for evaluating $\dfrac{\int_0^{1.0} \int_0^{y} \frac{dy}{M^2T'}\, dy}{\int_0^{1.0} \frac{dy}{M^2T'}}$.

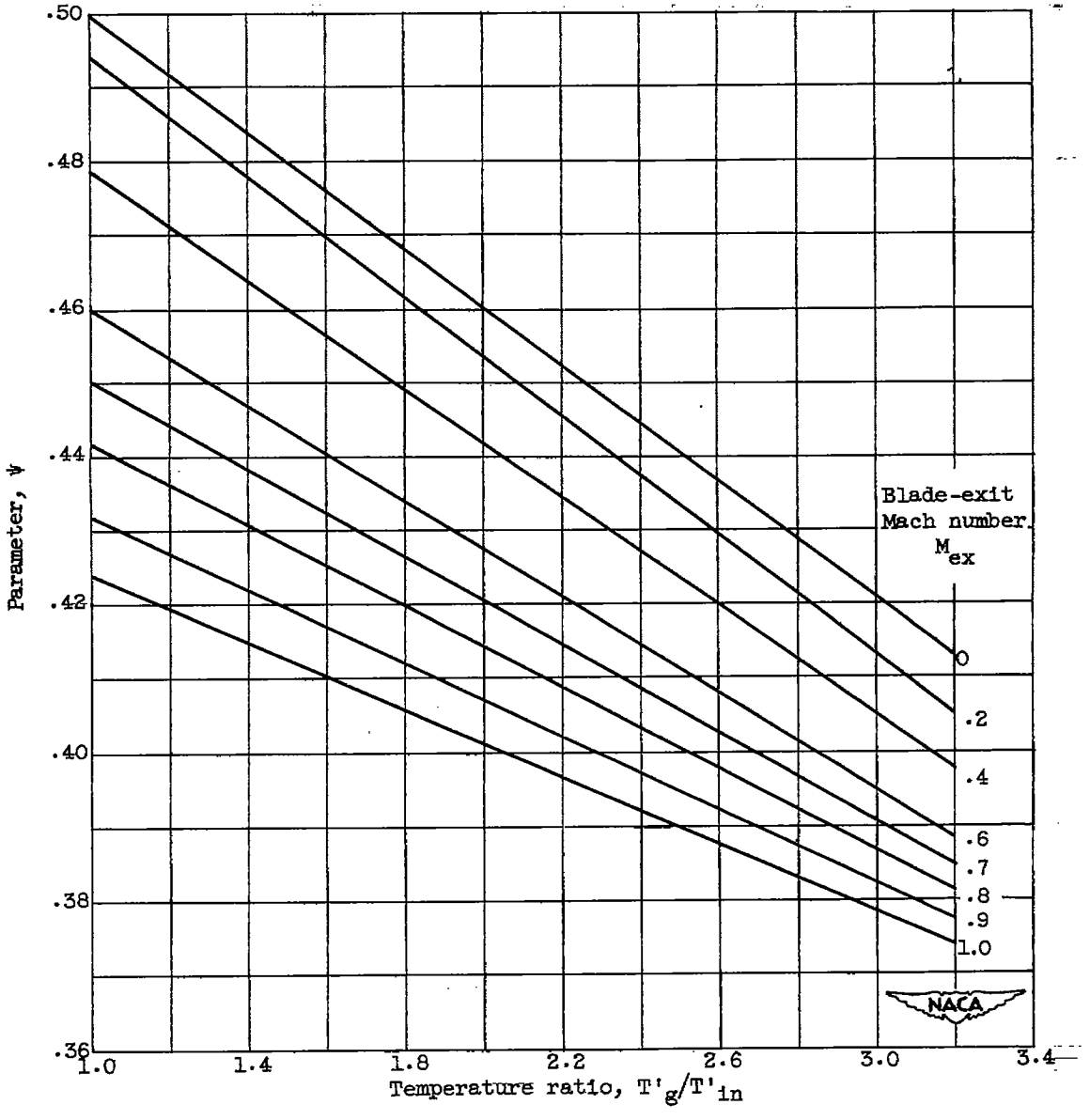

(b) Various Mach numbers.

Figure 9. - Concluded. Chart used for evaluating $\dfrac{\int_0^{1.0}\int_0^{y}\frac{dy}{M^2T'}\,dy}{\int_0^{1.0}\frac{dy}{M^2T'}}$.

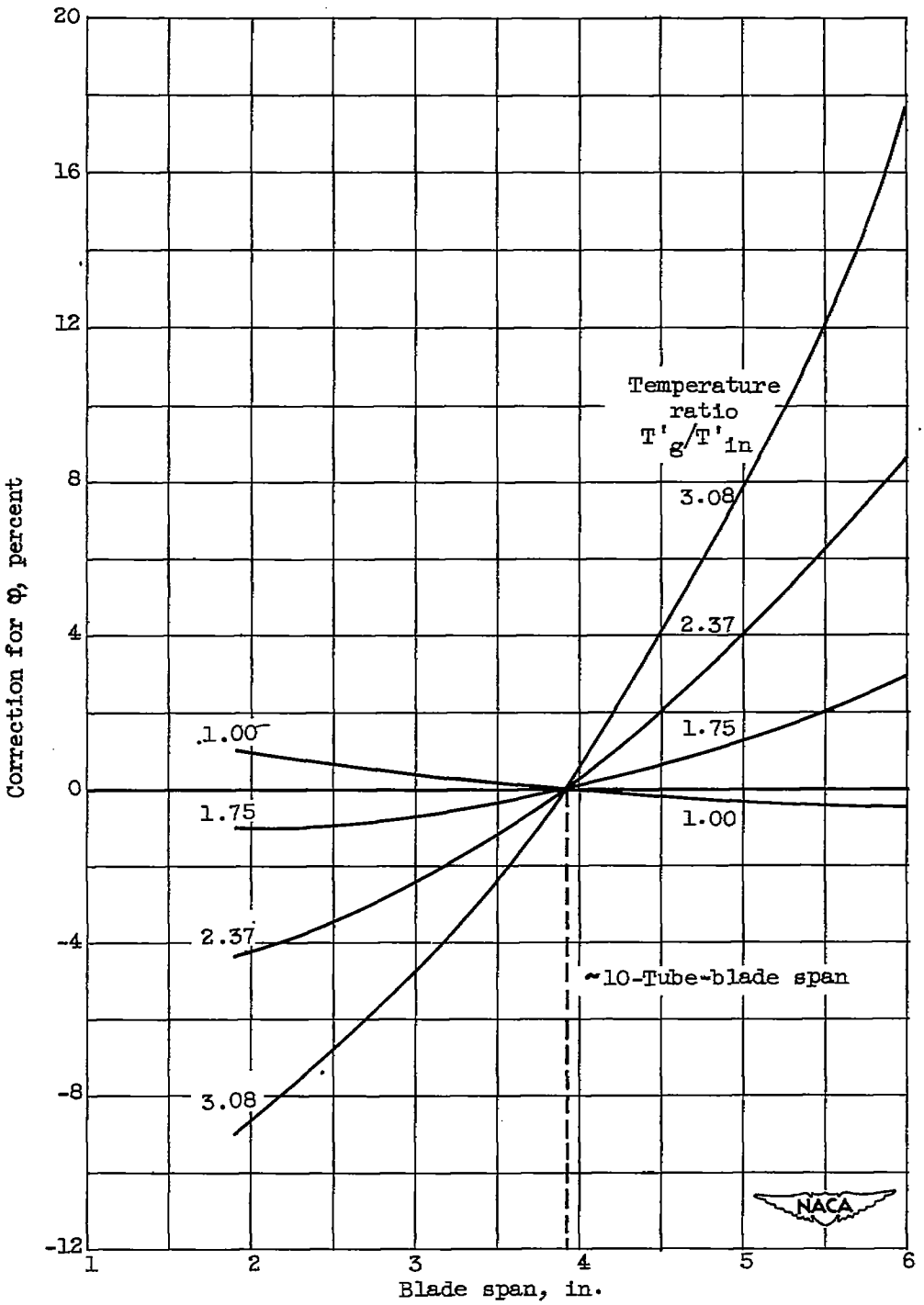

Figure 10. - Effect of blade span on parameter φ for constant outside heat-transfer coefficient H_o of 136 Btu per hour per square foot per °F.

[redacted]

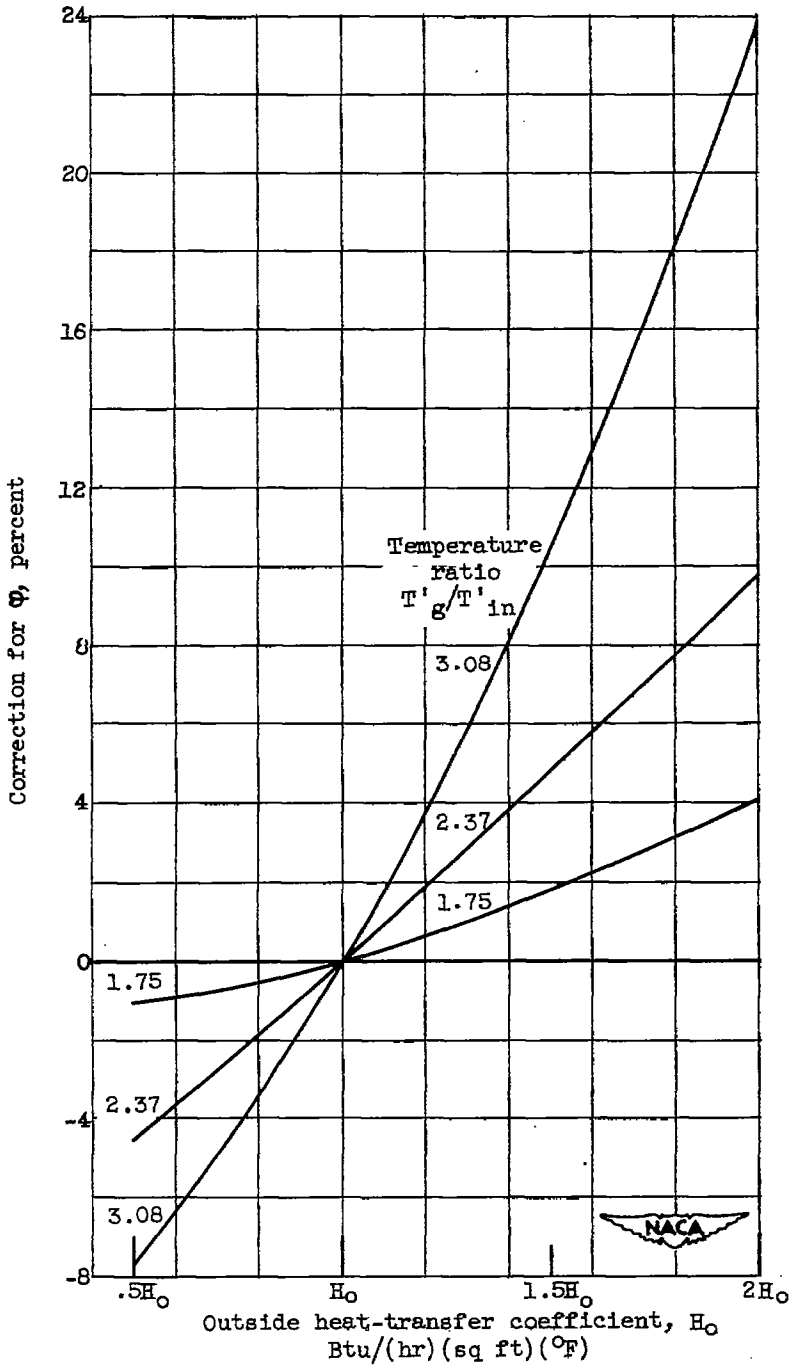

Figure 11. - Effect of outside heat-transfer coefficient on parameter Φ for constant blade span b_B of 3.92 inches. Outside heat-transfer coefficient, H_o, 136 Btu per hour per square foot per °F.

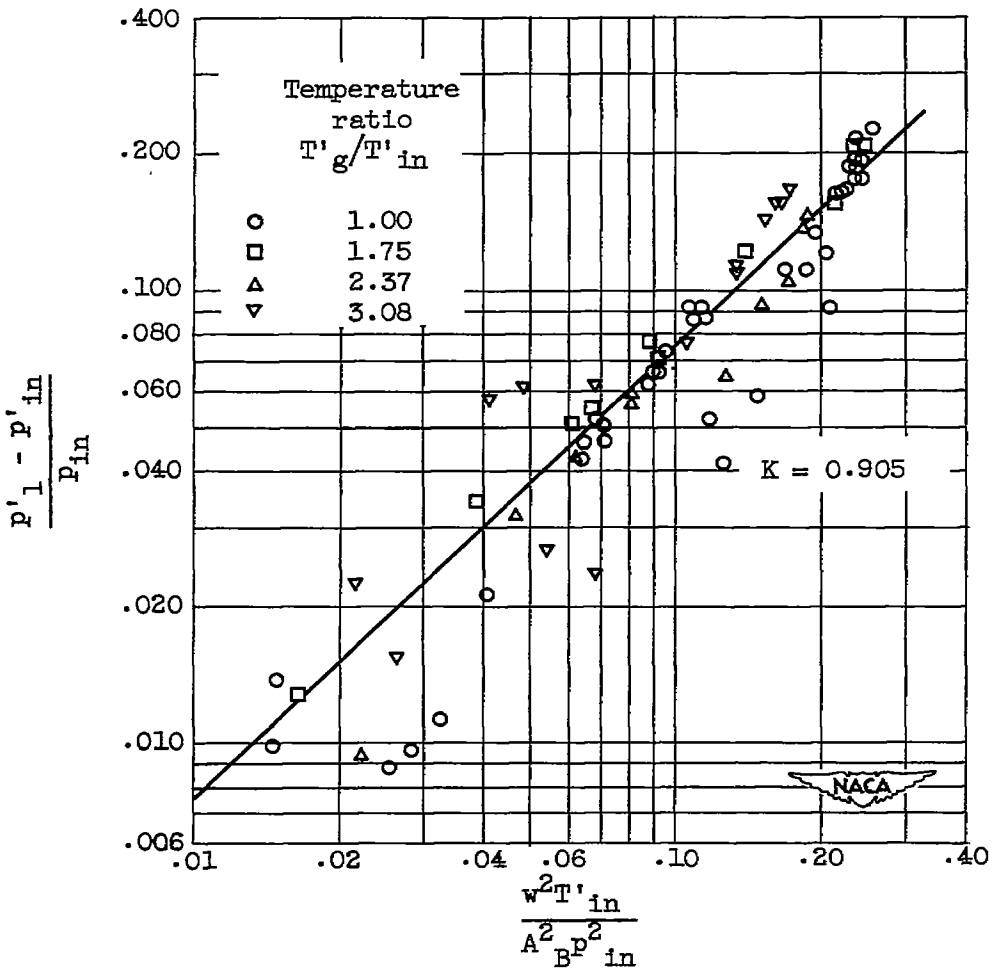

Figure 12. - Curve used for obtaining entrance loss coefficient K in entrance section of 10-tube blade.